AD-A153 842 RESONANT CARS DETECTION OF OH RADICALS(U) UNITED TECHNOLOGIES RESEARCH CENTER EAST HARTFORD CT J F VERDIECK ET AL. 31 JAN 85 UTRC/R85-955655 1/1

UNCLASSIFIED AFOSR-TR-85-0385 F49620-81-C-0063 F/G 7/4 NL

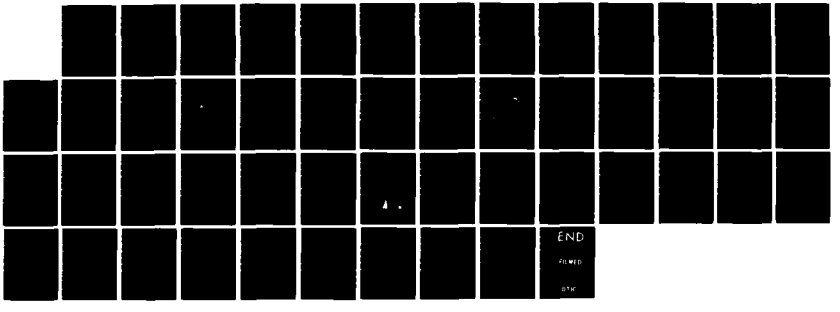

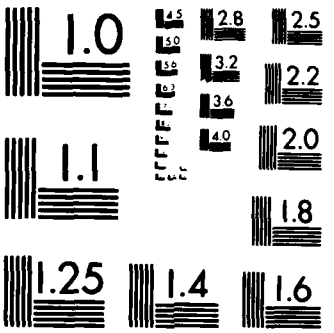

MICROCOPY RESOLUTION TEST CHART
NATIONAL BUREAU OF STANDARDS-1963-A

(2)

RESONANT CARS DETECTION OF OH RADICALS

FINAL REPORT
AFOSR CONTRACT NO. F49620-81-C-0063

REPORTED BY
JAMES F. VERDIECK, ROBERT J. HALL, AND ALAN C. ECKBRETH

21 Jan. 1985

ABSTRACT

(Coherent Anti-Stokes Raman Spectroscopy)

Under this AFOSR contract, resonant CARS of OH has been observed for the first time. Resonant CARS was achieved for several different electronic transitions in the ultraviolet A--X bands of OH in a methane/oxygen flame. Saturation of the resonant CARS spectrum of OH was examined experimentally and definite evidence found, both in the intensity variation, and the number and shapes of the lines. Concurrently with the experimental studies, a good understanding of the theoretical aspects of the resonant CARS process has been secured, to the extent that predicted resonant CARS spectra can be computer synthesized and graphed for any selected excitation frequency. A major departure from theoretical predictions was the experimental observation of satellite lines about the central line, not predicted from theory. At present, the cause of these extra resonances has not been determined, but their appearance may arise from saturation effects, or be caused by an undetermined nonlinear optical effect (such as dephasing-induced coherences). Another contributing factor may be rotational energy level transfer brought about by collision processes, occurring within the duration of the 10 nanosecond laser pulse. Through the use of the resonant CARS spectrum, a preliminary study of the variation of OH concentration was carried out as a function of the height of the CARS probe volume in the flame. This semi-quantitative experiment demonstates that resonant CARS offers potential for measuring the concentration of OH in combustion environments, even for the saturated case.

OBJECTIVES

Coherent anti-Stokes Raman spectroscopy (CARS) is a proven diagnostic for fundamental, research scale studies, as well as application to large-scale, working devices in divers fields ranging from combustion to chemical lasers and chemical processing. CARS offers a remote, non-perturbing method for accurately measuring temperature and species concentration with excellent spatial and temporal resolution. However, conventional CARS is limited to the detection of major species, 1 % or greater, at one atmosphere; unfortunately, radical concentrations are typically 0.1 % or less. An additional problem, specific to OH, is that there is spectral interference with the water CARS spectrum which overlaps the OH CARS spectrum.

The major goal of the this program has been to determine if the highly successful and convenient CARS diagnostic methods can be extended to the measurement of minority species such as radicals. The OH radical, so critically important to combustion chemistry, was chosen for study. The means of achieving the necessary sensitivity proposed was to employ resonant CARS. Electronically resonant CARS, or simply, resonant CARS, is achieved when one (or more) of the three CARS frequencies, the pump, the Stokes, or the CARS anti-Stokes frequency, is chosen to be resonant with an electronic transition of the molecule under investigation. When this electronic resonance condition is satisfied, enhancement factors of several orders of magnitude may be obtained, which in turn should permit the detection of minority species, such as ions, atoms, and radicals, like OH.

Under this contract, the first observation of resonant CARS from OH has been made in a methane/oxygen diffusion flame, under varying conditions, for several different choices of the electronic resonant frequency in the X -- A bands. Concurrently with the experimental studies, a good understanding of the theoretical aspects of resonant CARS has been gained, so that predicted resonant CARS spectra can be computer-synthesized and plotted. A rather complete description of these experimental and theoretical results can be found in Ref. 1. A more abbreviated account is given in Ref. 2. Both of these papers are attached to this report as Appendices 1 and 2, and may be referred to for a more detailed exposition of both theory and experiment.

UNCLASSIFIED

SECURITY CLASSIFICATION OF THIS PAGE

REPORT DOCUMENTATION PAGE

1a. REPORT SECURITY CLASSIFICATION: UNCLASSIFIED	1b. RESTRICTIVE MARKINGS
2a. SECURITY CLASSIFICATION AUTHORITY	3. DISTRIBUTION/AVAILABILITY OF REPORT: Approved for public release, distribution unlimited
2b. DECLASSIFICATION/DOWNGRADING SCHEDULE	
4. PERFORMING ORGANIZATION REPORT NUMBER(S): R85-955655	5. MONITORING ORGANIZATION REPORT NUMBER(S): AFOSR-TR- 85-0385
6a. NAME OF PERFORMING ORGANIZATION: United Technologies Research Center; 6b. OFFICE SYMBOL (If applicable)	7a. NAME OF MONITORING ORGANIZATION: Air Force Office of Scientific Research/NA
6c. ADDRESS (City, State and ZIP Code): Silver Lane, East Hartford, CT 06108	7b. ADDRESS (City, State and ZIP Code): Bolling AFB DC 20332-6448
8a. NAME OF FUNDING/SPONSORING ORGANIZATION: AIR FORCE OFFICE OF SCIENTIFIC RESEARCH; 8b. OFFICE SYMBOL (If applicable): NA	9. PROCUREMENT INSTRUMENT IDENTIFICATION NUMBER: F49620-81-C-0063
8c. ADDRESS (City, State and ZIP Code): Bolling AFB DC 20332-6448	10. SOURCE OF FUNDING NOS.

PROGRAM ELEMENT NO.	PROJECT NO.	TASK NO.	WORK UNIT NO.
61102F	2308	A3	

11. TITLE (Include Security Classification): Resonant CARS Detection of OH RADICALS

12. PERSONAL AUTHOR(S): J. F. Verdieck, R. J. Hall, A. C. Eckbreth

13a. TYPE OF REPORT	13b. TIME COVERED	14. DATE OF REPORT (Yr., Mo., Day)	15. PAGE COUNT
Final	FROM 8/1/81 TO 12/31/84	1985 January 31	9

16. SUPPLEMENTARY NOTATION

17. COSATI CODES			18. SUBJECT TERMS (Continue on reverse if necessary and identify by block number)
FIELD	GROUP	SUB GR.	Combustion Diagnostics, CARS, Resonant Enhancement Hydroxyl Radical

19. ABSTRACT (Continue on reverse if necessary and identify by block number)

Under this AFOSR contract, resonant CARS of OH has been observed for the first time. Resonant CARS was achieved for several different electronic transitions in the ultraviolet A--X bands of OH in a methane/oxygen flame. Saturation of the resonant CARS spectrum of OH was examined experimentally and definite evidence found, both in the intensity variation, and the number and shapes of the lines. Concurrently with the experimental studies, a good understanding of the theoretical aspects of the resonant CARS process has been secured, to the extent that predicted resonant CARS spectra can be computer synthesized and graphed for any selected excitation frequency. A major departure from theoretical predictions was the experimental observation of satellite lines about the central line, not predicted from theory. At present, the cause of these extra resonances has not been determined, but their appearance may arise from saturation effects, or be caused by an undetermined nonlinear optical effect (such as (CONT'D)

20. DISTRIBUTION/AVAILABILITY OF ABSTRACT	21. ABSTRACT SECURITY CLASSIFICATION
UNCLASSIFIED/UNLIMITED ☒ SAME AS RPT. ☐ DTIC USERS ☐	UNCLASSIFIED

22a. NAME OF RESPONSIBLE INDIVIDUAL	22b. TELEPHONE NUMBER (Include Area Code)	22c. OFFICE SYMBOL
LEONARD H CAVENY	(202) 767-4937	AFOSR/NA

DD FORM 1473, 83 APR — EDITION OF 1 JAN 73 IS OBSOLETE

UNCLASSIFIED

SECURITY CLASSIFICATION OF THIS PAGE

19. ABSTRACT (CONT'D)

dephasing-induced coherences). Another contributing factor may be rotational energy level transfer brought about by collision processes, occurring within the duration of the 10 nanosecond laser pulse. Through the use of the resonant CARS spectrum, a preliminary study of the variation of OH concentration was carried out as a function of the height of the CARS probe volume in the flame. This semi-quantitative experiment demonstrates that resonant CARS offers potential for measuring the concentration of OH in combustion environments, even for the saturated case.

THEORETICAL

The development of the theory of resonant CARS at UTRC under this contract was composed of several phases. It was realized initially, that in addition to understanding the resonant CARS process, the basic spectroscopy--electronic, vibrational, and rotational--of the OH radical had to be well-understood and catalogued. This was of great value to the experimental program, because the ability to model and synthesize the full rotational band of an chosen vibronic transition as a "stick" spectrum permitted the resonant excitation frequencies to be intelligently chosen. This capability required a knowledge of the vibration-rotation constants and the transition dipole moments for the electronic transitions of interest. This information was further employed for the calculation of the resonant CARS spectrum. The resonant CARS spectra calculated from theory are quite simple in appearance, consisting of only three lines. This is true because the resonant CARS process selects (in much the same manner as a delta function) only a small number of possible allowed transitions. The allowed rovibronic transitions for OH are P,Q, and R. Full details of the theory are presented in Ref. 1. The possibility of finding so-called double and triple resonance in OH was considered theoretically and a computer search for these coincidences was made. Because of the large rotational line spacing in OH, it was realized that such possibilities were rare; this was borne out by the computer search. For each of the experimental resonances found (described below), a theoretical spectrum was calculated (examples are shown in Refs. 1, 2) for comparison. The issue of saturation, because of its complexity, was not addressed theoretically; however, experimental evidence of saturation was found and is discussed below.

EXPERIMENTAL

Several important factors were considered in the design of a resonant CARS experiment which must detect a molecular free radical in the gas phase. The problems are compounded by the fact that the OH electronic transitions lie in the ultraviolet. This requirement of working in the UV introduced the additional complexities of frequency doubling two narroband tunable dye lasers(both pumped by the limited output of a frequency-doubled Nd:YAG laser), manipulating and detecting ultraviolet beams, and dealing with dichroic mirrors and filters that were only partially effective in removing unwanted wavelengths, while at the same time, severely attenuating the desired wavelength.

The configuration conventionally employed for resonant CARS makes use of two tunable, narrowband dye lasers, one of which (the pump laser frequency) is tuned to the selected electronic resonance and held fixed, and the second (Stokes laser frequency) slowly scanned in frequency, thereby generating the resonant CARS spectrum. The two tunable narrowband lasers are synchronously driven with the second harmonic (532 nm) of a pulsed neodymium YAG (Nd:YAG) laser operating at 10 Hz. One of the dye lasers (Stokes) is a commercial unit which can be scanned at various speeds. The pump laser is homemade, of the Littmann grazing-grating configuration. Each dye laser produces radiation of frequency width less than 0.3 wavenumber and the energy per pulse between 10 and 20 mJ, depending upon the laser dye chosen.

The laser output from both dye lasers must be frequency doubled to achieve resonance on the OH X--A bands which lie in the ultraviolet. The pump dye laser is frequency doubled with a manually adjusted second harmonic crystal. Because the Stokes laser is scanned, an automatic angle-tuned device which maintains constant output power of the second harmonic frequency as the fundamental is tuned, must be employed. A WEX-1 (Quanta-Ray) performs this task over the fundamental dye laser spectrum at scan rates in excess of 0.05 nm/sec. The second harmonic conversion efficiency appears to be about 10 % for both lasers; hence, ultraviolet energies range between 1 and 2 millijoules per pulse, corresponding to peak powers of 100 to 200 kilowatts.

The two ultraviolet laser beams (pump and Stokes) are combined with a dichroic mirror and focussed into the methane/oxygen flame in the collinear CARS geometry. The beams emerging from the flame, now containing the CARS frequency also, are recollimated and directed to the detection system. The pump and Stokes beams are partially removed with a dichroic mirror and trapped. Because the dichroic is unsuccessful in completely removing the undesired frequencies, the three emergent beams are spatially separated with a dispersing prism and only the desired CARS frequency allowed to enter the detector, a filtered photomultiplier. One of the most essential features of the experiment is an emission/fluorescence detection arm at right angles to the CARS laser beams. This segment of the apparatus served to calibrate a monochromator through the known emission spectrum of the OH radical. More importantly, this subsystem served both to indicate when a resonance excitation has been found, and to identify the particular transition in question through the unique laser-induced fluorescence spectrum. The disposition of the optical configuration of the experiment is best appreciated by reference to the experimental figures of Appendix 1 or 2.

The burner used throughout these studies consisted of a staggered array of stainless steel capillary tubes (0.125 o.d.) which were ground flush with an edge-cooled brass plate which held the tubes in place. The matrix of alternating fuel/oxidizer tubes was surrounded by an outer layer of tubes

which provided a nitrogen sheath to stabilize the flame. The burner produced a flame of very uniform appearance. Mounted on a vertical translation stage, the burner could be moved relative to the CARS laser beams.

RESULTS

The first demonstration of resonant CARS in OH was obtained with the pump frequency resonant on the P1(9) rotational line of the 1-0 vibronic band. The spectrum (a scanned CARS spectrum) was obtained by scanning the Stokes laser, while recording the change in intensity of the CARS signal falling on the filter detector. Several spectra are displayed in Appendices 1 and 2. In addition to the OH resonant CARS spectrum, the "normal" CARS spectrum of water was easily observed because of its great abundance in the particular flame employed. The band head of the water CARS spectrum is a very distinctive feature and provides a frequency marker for calibrating spectra. When the pump frequency is carefully adjusted to the peak of the resonant transition, the water CARS spectrum is barely discernible in comparison to the OH resonant CARS spectrum. This was taken as prime evidence that resonanat CARS was being observed, because the water concentration is at least four to five times that of OH in the methane/oxygen flame, the normal CARS spectrum of OH would be much less than that of the water CARS, probably totally lost in the water CARS band. The enhancement factor obtained through the resonant CARS process not only makes the OH signal observable, but much larger than the water signal. The enhancement factor for the OH resonant CARS may be larger than is apparent, because the true scaling of the CARS signal involves a consideration of linewidths and constructive/destructive interferences between the lines which has not been factored in.

The first resonant CARS spectra obtained (for large values of the rotational quantum number, P1(9) and Q1(14)) are incomplete with respect to the theoretically predicted resonant CARS spectra because the outermost lines are not observed in the experiment, mainly because of the limited spectral tuning range of the Stokes dye laser. The spacing between the outermost lines depends directly upon the rotational quantum number; hence, these lines will move toward each other as this quantum number decreases. For resonances on Q1(4) and Q1(2), evidence for the outermost components was observed.

A preliminary exploration of saturation was made by reducing the intensity of the pump beam with fused silica flats and partially reflecting UV mirrors, resulting in an attenuation of 5.5. In order to obtain reasonable signal strength, the gain had to be increased by a factor of ten. Because the CARS signal scales as the square of the pump laser power, a reduction of 30 should have been seen. This discrepancy, along with the change in shape and number of

lines was interpreted as evidence that saturation effects must be considered. A more thorough study is called for; one which includes attenuation of the Stokes laser beam to determine if both of the input laser beams contribute to saturation of the resonant CARS process, and how that affects the resultant CARS spectra.

The sensitivity of the resonant CARS spectrum to changes in concentration was studied by changing the height of the incident CARS laser beams relative to the height of the burner surface. The results showed that the OH CARS signal was much larger than the water signal near the burner surface (0.5 cm), but nearly disappeared at a height of 2.0 cm, where the water CARS signal was much stronger. Future studies will involve a detailed calibration of the concentrations of both OH and water throughout the flame, as well as the temperature distribution, so that resonant CARS as a quantitative diagnostic may be properly assessed. Saturation may prove to be a problem for quantitative measurements; however, even in the case of saturation, it may be possible to construct a calibrated working curve of concentration versus signal strength, as is done in analytical chemistry for spectrophotometry, when there is a failure of Beer's law.

A significant disparity between theory and experiment was observed in that the experimental spectra display a group of unpredicted satellite lines about the strong central peak. These lines number from 2 or 3, up to as many as 7 (this may be a function of the signal-to-noise ratio), and have varying types of lineshapes (dispersion, absorption, or a combination of the two). The origin of these extra lines may be a strong-field effect, i.e., saturation, which was not treated in the theoretical analysis. Several recent theoretical analyses of resonant CARS in the strong field regime have predicted the appearance of satellite line structure about the central line with a frequency separation given by the Rabi frequency. Other explanations of extra resonances involve "dephasing-induced" effects. A third possibility may be rotational energy transfer from the resonance level excited by the resonant pump beam. Population in adjacent excited states could then cause additional resonances as the Stokes laser is tuned. A fourth possibility is that more than one transition are simultaneously excited due to the base width of the pump laser.

Another interesting question is the appearance of the resonant CARS spectrum as the pump laser frequency is parametrically tuned through the electronic resonance. Dramatic changes are observed as to the number, shape and relative intensity distribution of the lines of the spectrum, for small changes in tuning. This extreme sensitivity to tuning has been observed by other workers in the field of resonant CARS. The cause of such sensititivity derives from the very nature of the resonant CARS process and it cannot be avoided. What it does imply is that one must employ very narrowband dye lasers which can be tuned very precisely to the transition line center. Obviously these

considerations bear heavily upon the problems listed in the previous paragraph. Answers to these questions, and others are presently being pursued under a new, one-year AFOSR Contract which has just started.

CONCLUSIONS

Electronically resonant CARS of the OH radical has been demonstrated in a very hot methane/oxygen flame. The resonant CARS spectrum was generated by use of two frequency-doubled, pulsed, narrowband dye lasers, one of which was tuned and then fixed on a selected OH X--A transition, while the other was scanned over the appropriate range. The OH resonant CARS signal is strong compared to the water CARS spectrum, even though water is much more abundant than OH in the flame. Resonant CARS was observed from several different electronic resonances and was quite sensitive to precise tuning of the pump laser frequency. The theory of resonant CARS in the OH radical has been treated and the predicted appearance of OH resonant CARS spectra presented. Saturation, for which there is some experimental evidence, has not been included in the theory. Agreement between theory and experiment is good, except for the experimental observation of satellite structure about the central line. This additional structure is believed to arise from collisional redistribution of population in rotational energy levels of the upper electronic state, or from saturation effects. The variation of the resonant CARS spectrum as a function of the laser beam height in the flame was observed and offers promise that resonant CARS may be applicable to quantitative measurements of concentration.

ACKNOWLEDGEMENTS

The authors wish to acknowledge valuable discussions with Prof. Nicolaas Bloembergen of the Harvard University Physics Department, and with Dr. David R. Crosley of SRI International, Inc. Thanks are also due Edward Dzwonkowski and Normand Gantick for assistance with the experiments.

REFERENCES

1. Verdieck, J.F., R.J. Hall, and A.C. Eckbreth, "Electronically Resonant CARS Detection of OH," Paper AIAA-83-1477, AIAA 18th Thermophysics Conference, Jun 1-3, 1983, Montreal, PQ, Cananda.

2. Verdieck, J.F., R.J. Hall, and A.C. Eckbreth, "Electronically Resonant CARS Detection of OH," in Combustion Diagnostics by Nonintrusive Methods, edited by Jeffrey A. Roux and T. Dwayne McCay, Vol. 92 of Progress in Astronautics and Aeronautics, 1984.

INTERACTIONS (COUPLING ACTIVITIES)

During this contract, the following presentations were given:

1. "Resonant CARS Detection of the OH Radical," James F. Verdieck, Robert J. Hall, and Alan C. Eckbreth, presented by J.F. Verdieck at 1982 AROSR Research Meeting on Diagnostics of Reacting Flows, Stanford University, 25-26 February 1982

2. "Resonant CARS Detection of OH Radicals," by J.F. Verdieck and A.C. Eckbreth, presented by J.F. Verdieck at the 1983 AFOSR/AFRPL Rocket Propulsion Meeting, Lancaster, CA, 1-3 March 1983

3. "Electronically Resonant CARS Detection of OH Radical" by J.F. Verdieck and A.C. Eckbreth, presented by J.F. Verdieck, Paper No. WD 3, CLEO '83, Baltimore, MD, 17-20 May 1983

4. "Electronically Resonant CARS Detection of OH," by J.F. Verdieck, R.J. Hall, and A.C. Eckbreth, Paper No. AIAA 83-1477, AIAA 18th Thermophysics Conference, Montreal, Que., 1-3 June 1983

5. "Combustion Analysis under Difficult Conditions: Applied CARS Spectroscopy" Invited Paper presented by J.F. Verdieck at the American Chemical Society Northeast Regional Meeting (NERM-13), Hartford, CT, at the University of Hartford, 26-29 June 1983

6. "CARS and LIF Combustion Diagnostics," Combustion Course Seminar delivered by J.F. Verdieck at Rensselaer Polytechnic Institute Chemical Engineering Department, Troy, NY, 14 October 1983

7. "Resonant CARS of the Hydroxyl Radical" Paper delivered by J.F. Verdieck at Lasers '83 Conference (SOQUE), San Francisco, CA, 12-16 December 1983

8. "Combustion Diagnostics with CARS and LIF" Seminar given by J.F. Verdieck to The Chemical Society of McGill University, Montreal, PQ, Canada, 10 January 1984

9. "Resonant CARS Detection of OH Radicals" James F. Verdieck, Robert J. Hall, and Alan C. Eckbreth, given by J.F. Verdieck at the AFOSR Research Meeting on Diagnostics of Reacting Flows, Yale University, 21-22 March 1984

10. "Exciplex Systems for Real Time Visualization of Fuel Sprays" L.A. Melton and J.F. Verdieck, presented by J.F. Verdieck at the 1984 AFOSR/ONR Contractors Meeting on Airbreathing Combustion Research, Carnegie-Mellon University Department of Mechanical Engineering, Pittsburgh, PA 20-21 June 1984

11. "Electronically Resonant CARS Detection of OH" Poster Paper 63, Session G-2, Combustion Diagnostics, given by J.F. Verdieck, XXth International Symposium on Combustion, Ann Arbor, MI 12-17 August 1984

AIAA'83

AIAA-83-1477

Electronically Resonant CARS Detection of OH

J.F. Verdieck, R.J. Hall, and A.C. Eckbreth,
United Technologies Research Center,
East Hartford, CT

AIAA 18th Thermophysics Conference

June 1-3, 1983
Montreal, Canada

ELECTRONICALLY RESONANT CARS DETECTION OF OH*

James F. Verdieck, Robert J. Hall and Alan C. Eckbreth
United Technologies Research Center
East Hartford, Connecticut 06108

Abstract

CARS (coherent anti-Stokes Raman spectroscopy) is a nonlinear spectroscopic technique capable of making remote, highly accurate measurements of temperature and concentration which are both temporally and spatially precise, in extremely difficult environments such as internal combustion engines and gas turbine exhausts. A major disadvantage of CARS methods is that its application is generally limited to those species whose concentration is on the order of one percent or greater. In order to extend CARS detectivity, electronically, resonantly-enhanced CARS can be employed, whereby one of the CARS laser frequencies is selected to be resonant with an electronic transition. This results in a large signal enhancement (possibly seveveral orders of magnitude). In this paper, the results of applying resonant CARS to the detection of the hydroxyl radical in a methane/oxygen flame will be presented. The theory of electronically resonant CARS, predicted spectra, and the experimental procedure are described. The variation of the experimentally obtained resonant CARS spectrum with different choices of electronic resonance is shown. A preliminary demonstration of saturation is also illustrated, as is the correlation of the resonant CARS spectrum with dependence of OH concentration on flame height.

*The authors wish to thank the United States Air Force Office of Scientific Research for partial support of this research through Contract No. F49620-81-C-0063

Introduction

CARS (coherent anti-Stokes Raman spectroscopy) is a nonlinear optical process wherein three optical fields are combined in a material medium to generate a fourth optical field. As conventionally employed, two laser frequencies, ω_1 (the pump beam) and ω_2 (the Stokes beam), are mixed to produce the CARS frequency, ω_3, which appears as a coherent, collimated beam. This is illustrated in Fig. 1a. The CARS signal is large and easily detected (even in the prescence of particles or a highly luminous background) when the frequency difference between the two input frequencies corresponds to a Raman-active molecular vibration or rotation (or an electronic) transition . Because CARS is a coherent, nonlinear process, laser beams are required to provide the proper phases of the optical fields in time and space, and the high intensity to enhance the nonlinear aspect of the process. Usually, high-peak power pulsed lasers are employed to generate CARS, particularly for combustion diagnostic applications. Photon energy is conserved in the CARS process(in contrast to the Raman effect), as illustrated in Fig. 1b. Note that $\omega_1 > \omega_2$. Fig. 1c exhibits two distinct methods of generating a CARS spectrum. One of these methods is to employ a broadband (100 cm^{-1} wide) Stokes laser, which results in the generation of the entire CARS spectrum of interest from each laser shot. This particular method is very useful for combustion diagnostics because single-shot (typically 10 nanoseconds) thermometry can be performed. The second method uses two narrowband lasers and tunes one of these, generating the CARS spectrum by scanning. It is this second, scanned technique which is utilized to generate resonantly enhanced CARS, by scanning ω_2 while holding ω_1 fixed on an electronic transition.

CARS applications are diverse and too numerous to catalogue in detail here. It is an important spectroscopic technique well-suited for fundamental studies of molecules, large and small. CARS has been repeatedly demonstrated to be a su-

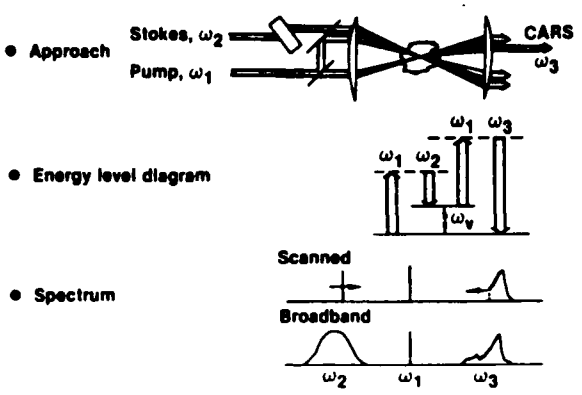

Fig. 1 Basic scheme for CARS spectroscopy.

perior technique for remote diagnostics for combustion research, on both a laboratory scale and for large-scale practical devices. Examples include CARS temperature and concentration measurements in sooty flames,[1] plasmas,[2] internal combustion engines[3] and gas turbine engines.[4] The theory and application of CARS have been extensively reviewed; these reviews may be consulted for detailed descriptions.[5-7]

A major disadvantage of CARS diagnostic methods is that, at atmospheric pressure, they are generally limited in application to species whose concentration is about one percent or greater. A means of overcoming this limitation is to enhance the CARS signal through electronic resonance. Recall that the normal CARS process is vibrationally resonant; if in addition, one of the input CARS frequencies is resonant with an electronic transition, a large increase in the CARS signal occurs. This increase can be a factor of several hundred over the normal CARS effect. Electronically-resonant CARS(resonant CARS for short) has been observed for several large molecules in solution phase; however, to date, only a limited number of molecules have been studied using resonant CARS in the gaseous phase, namely I_2,[8] NO_2,[9] and most recently, C_2.[10] The reason for this limited application in the gas phase is clear; there are very few simple, small molecules which absorb visible light (where dye lasers work efficiently). Indeed, the last cited case, C_2, is a radical which must be generated in a flame or a microwave discharge.[10]

The hydroxyl radical was chosen for study at this laboratory because of its ubiquitous presence and extreme importance in combustion chemistry. OH enters into the oxidation mechanisms of nearly all hydrogen-containing fuels. OH plays an essential role in the mechanisms of the oxidation mechanisms of nearly all types of hydrocarbons. Hydroxyl radical reactions are usually very rapid (because OH is a radical, activation energies are small) and OH often enters into explosive chain reactions. OH is also important in atmospheric chemistry and has been implicated in acid rain formation from nitrogen and sulfur oxides. For these important reasons, it is desirable to be able to detect and measure the concentration of the OH radical in difficult environments.

Optical methods presently employed to measure OH concentrations are UV absorption spectroscopy and laser-induced fluorescence spectroscopy (LIFS).[11] The absorption method is readily applied and useful where spatial resolution is not required. Even where applicable, gradient and edge effects can degrade absorption measurement accuracy. LIFS is a point measurement technique which enjoys good success in carefully controlled laboratory devices operating cleanly at low pressure. However, in practical combustion environments, fluorescence methods can suffer from interferences, such as fluorescence from other species and from laser-induced particle incandescence. The major problem with fluorescence techniques is collisional quenching, particularly for application in high pressure devices. In contrast, CARS diagnostic measurements have been demonstrated in several practical combustion systems such as highly luminous sooting flames, internal combustion engines, gas turbine combustors, solid propellant flames, and alumina particle laden flows. Because CARS methods have proven superior in these types of environments, it is beneficial to extend the sensitivity for CARS to radicals such as OH.

In the sections which follow, the progress on application of resonant CARS to the detection of OH is described. The effort at UTRC has been and continues to be a combined theoretical and experimental program. The first section is a basic primer on OH spectroscopy, required for application of resonant CARS. Following this section is a presentation of the theory of resonant CARS with predicted resonant CARS spectra for comparison with experimental spectra. Issues of saturation and rotational state redistribution have not yet been considered because of their difficulty. A description of the experimental apparatus employed follows the theoretical section. The results of the experiments to date are presented mainly through display of the resonant CARS spectra obtained from different resonances, variation of incident laser power, and laser beam height changes relative to the burner surface. Conclusions and plans for future studies are given in the final section.

Spectroscopy of the Hydroxyl Radical

It is essential to understand the electronic, vibrational, and rotational aspects of OH spectroscopy in order to wisely select the resonant CARS pump laser frequency, ω_1. Once ω_1 has been chosen, the Stokes frequency, ω_2, is determined by the OH vibrational shift. The spectral positions of the excitation frequencies, although a matter of some choice, depend strongly on the laser dyes available which yield high second-harmonic conversion efficiency in the appropriate region of the ultraviolet.

The spectroscopy of the OH radical is rather complicated for a diatomic molecule. This complexity arises mainly from the unpaired electron spin and the non-zero orbital angular momentum of the electronic ground state. Without going into fine detail, the result of spin-orbit coupling is a $^2\Pi$ electronic ground state which is split by about 126 cm^{-1}. This $^2\Pi$ state is inverted with the $\Omega = \pm 3/2$ state lying below the $\pm 1/2$ state. Following Dieke and Crosswhite,[12] these states are designated f_1 and f_2, respectively, and are shown along with the first excited state, $^2\Sigma$, in Fig. (2).

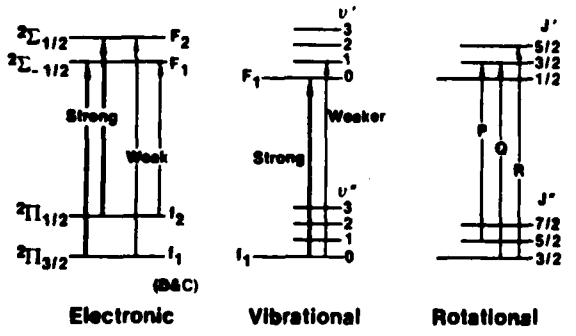

Fig. 2 Fundamental considerations for OH spectroscopy.

The splitting between the upper state components F_1 and F_2 is exaggerated to illustrate the strongly- vs weakly-allowed transitions from the ground electronic state (generic label, X) to the first excited state (A). Also shown in this figure are the vibrational and rotational transitions from X to A. There are no vibrational selection rules for electronic transitions, but the Franck-Condon principle governs the strength of the vibronic transitions as the middle figure indicates. Note that the convention on labeling states is v' for the upper state and v" for the lower. Moreover, a particular transition is designated as v', v", hence, the 1-0 vibronic transition implies a transition, in either absorption or emission, between v' = 1 of the A state and v" = 0 of the X state. For the case of $^2\Pi$ state, the rotational selection rule permits $\Delta J = 0, \pm 1$; therefore, Q, P and R rotational branches are observed as shown in Fig. (2). Note also that the quantum number J for this case is the total angular momentum; i.e., the sum of electronic angular momentum, Ω, and the mechanical angular momentum of the molecule, N. For this reason, J" is half-integral and has an initial value of 3/2.

If one excludes the rotational fine structure and examines only the vibronic structure of the X to A transition of OH, a plot of vibronic bandheads results, as shown in Fig. (3). This spectrum is

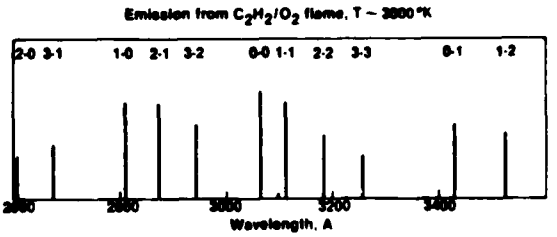

Fig. 3 Vibronic bandheads for the A to X transitions of OH. Adapted from Dieke and Crosswhite, Ref. 12.

extremely important because, in conjunction with Fig. (4), the relative output of conventional laser dyes, it was used to determine the optimum vibronic band for the resonant CARS pump frequency, ω_1. The choice of the 1-0 band was made because it places ω_1 in the region of the very efficient laser dye, 1, rhodamine 590, so that reasonable second harmonic power can be obtained. The Stokes frequency, ω_2, is required to lie in the range 3000 to 3500 cm^{-1} to the low frequency side (high wavelength) side of ω_1. According to Fig. (4), the laser dye 5, DCM, covers the required range nicely, with good energy conversion. It must be

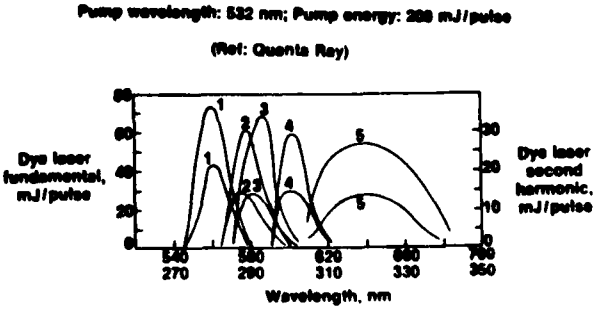

Fig. 4 Second harmonic conversion of some typical laser dyes.

noted that the 0-0 band, at 307 nm, much exploited for laser induced fluorescence, appears to be a poor choice for ω_1 because both of the laser frequencies would lie on the opposite edges of the DCM curve and the second harmonic power would be quite low.

The complete rotational structure of the 1-0 system is shown in Fig. (5). This is the superposition of the P, Q, and R branches arising from both components of the $^2\Pi$ electronic ground state. In order to distinguish these components a subscript 1 or 2 is used for transitions from or to the f_1 and f_2 states, respectively.

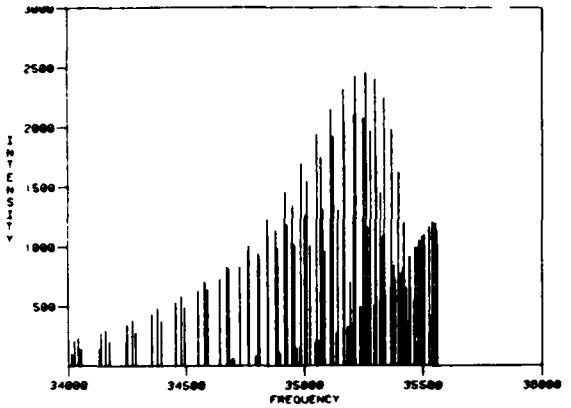

Fig. 5 Theoretical "stick" spectrum of the 1-0 band of OH. T = 3000°K

This notation is illustrated next in Fig. (6), which shows a portion of the 1-0 band greatly expanded. It is noted that there is considerable spacing, 5 to 10 cm^{-1}, between lines such as $Q_1(14)$ and and $P_1(9)$ in this region. In this region of the spectrum, 10 cm^{-1} corresponds to about 0.1 nm. The two lines mentioned were employed for the first observation of resonance CARS in OH.

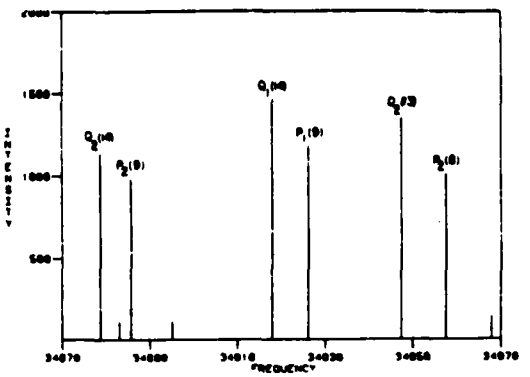

Fig. 6 High resolution "stick" spectrum of OH expanded about P_1 (9).

Resonant CARS Theory

The traditional approach to interpretation of resonance CARS spectra has been to employ the general, 48 term expression for the third-order electric susceptibility that has been derived by several authors.[8,13] This expression has been obtained either algebraically, using a perturbation expansion solution of the density matrix equation of motion, or diagrammatically, using "doubled" Feynman diagrams.

Both approaches yield equivalent results. The complete expression, showing all terms, has been presented by Bloembergen, Lotem, & Lynch.[13] Certain of the terms contain vibrationally resonant denominators which cause them to be large when the frequency difference between the pump and Stokes sources encroaches upon Raman-active vibrational modes. If all other terms are lumped into the nonresonant background susceptibility, χ_{NR}, then the third-order electric susceptibility may be expressed as a sum of this nonresonant term and a vibrationally resonant term which is a summation of contributions from all Raman-active modes, namely,

$$\chi^{(3)}(\omega_3) = \chi_{NR} + \sum_{a,b} \chi_R^{ba} \qquad (1)$$

where a and b represent the initial and final vibration-rotation quantum numbers of a particular Raman transition whose contribution to the resonant part of the susceptibility can be expressed as[8]

$$\chi_{ab}^{(3)} = \frac{N}{\hbar^3} \frac{1}{(\omega_{ba}-\omega_1+\omega_2-i\Gamma_{ba})} \left[\sum_{n'} \left(\frac{\mu_{an'}\mu_{n'b}}{\omega_{n'a}-\omega_3-i\Gamma_{n'a}} + \frac{\mu_{an'}\mu_{n'b}}{\omega_{n'b}+\omega_3+i\Gamma_{n'b}} \right) \times \sum_n (\rho_{aa}^{(0)} - \rho_{nn}^{(0)}) \left(\frac{\mu_{bn}\mu_{na}}{\omega_{na}+\omega_2-i\Gamma_{na}} + \frac{\mu_{bn}\mu_{na}}{\omega_{na}-\omega_1-i\Gamma_{na}} \right) \right.$$

$$\left. - \sum_{n'} \left(\frac{\mu_{an'}\mu_{n'b}}{\omega_{n'a}-\omega_3-i\Gamma_{na}} + \frac{\mu_{an'}\mu_{n'b}}{\omega_{n'b}+\omega_3+i\Gamma_{n'b}} \right) \times \sum_n (\rho_{bb}^{(0)} - \rho_{nn}^{(0)}) \left(\frac{\mu_{bn}\mu_{na}}{\omega_{nb}-\omega_2+i\Gamma_{nb}} + \frac{\mu_{bn}\mu_{na}}{\omega_{nb}+\omega_1+i\Gamma_{nb}} \right) \right] . \qquad (2)$$

In Eq. 2, N represents the OH number density, ω denotes frequency, Γ denotes pressure-broadened linewidth, $\rho^{(o)}$ Boltzmann population, and μ, electric dipole matrix element. n and n' represent excited electronic states of the molecule, and it is apparent from examination of the denominators in Eq. 2 that electronic resonant enhancement will occur if either ω_1, ω_2, or ω_3 coincides with an allowed electronic transition. It is also apparent that selecting the pump frequency resonant with a particular a-n electronic transition "picks out" a particular initial ground vibration-rotation state a, making it possible to ignore the contributions of all other initial Raman states in the ground electronic-vibrational manifold. Because the term which contains the denominator resonant in ω_2 is proportional to the population ρ_{bb} of the upper state in the Raman transition, it is reasonable to expect that its contribution will be small, particularly for a molecule like OH with a very large vibrational spacing. The rules for interpretation of resonant CARS spectra in terms of Eq. 2 have been discussed at length in the literature, with successful application to I_2,[8] N_2,[9] and C_2.[10]

One notes that if the pump frequency is made to coincide with the frequency of a particular electronic transition a-n, and the Stokes frequency is tuned to sweep out the range of Raman frequencies, there will be double resonances which occur when $\omega_1 - \omega_2 = \omega_{ab}$, or $\omega_3 = \omega_{an'}$, and the possibility of triple resonances when $\omega_1 = \omega_{an}$, $\omega_1 - \omega_2 = \omega_{ab}$, and $\omega_3 = \omega_{an'}$. The criterion for the occurrence of a triple resonance is that the transitions a-n and a-n' be optically allowed and that $\omega_{ab} = \omega_{nn'}$. While the triple resonances do occur in molecules like I_2 and C_2 with closely spaced vibration-rotation states, they are expected to be extremely improbable in a molecule like OH with very large spacing between levels. If two distinct pump sources with slightly different frequencies are employed, then a triple resonance can be achieved in OH, but in general they should not be expected.

The electronic and vibrational spectroscopy of OH has been discussed previously. In the electronic absorption or emission spectrum, P, Q, and R branches are allowed, making possible 12 branches. However, the six satellite branches in which the f_1 or f_2 designation changes will be relatively weak, leaving six main branches. In OH vibrational spectroscopy O, P, Q, R, and S transitions are allowed. The weakness of the satellite branches in the electronic spectrum means that vibrational transitions in which the f_1 or f_2 designation changes can also be ignored. By examination of Eq. 2 and considering the selection rules for electronic and vibrational transitions, which must be obeyed for the resonant CARS process, it is possible to specify the types of resonances which will give rise to the spectral features in electronically resonantly enhanced OH CARS. As an example, if ω_1 is tuned to a Q-branch transition, then P, Q, and R Raman resonances will be observed, and the anti-Stokes term will be contributed by a Q-transition. This is illustrated in Fig. 7.

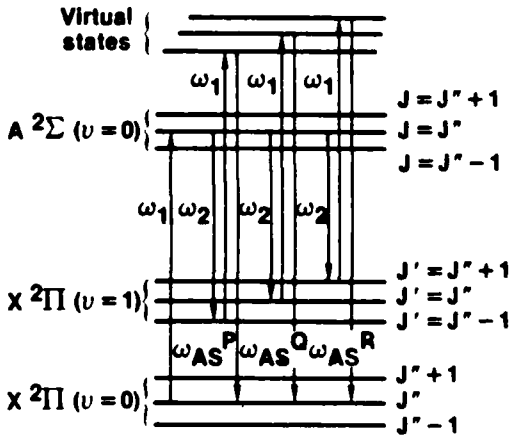

Fig. 7 Energy level diagram showing origin of resonant CARS triplet structure.

The general rules are:

Pump tuned to:	Allowed Raman resonances as Stokes is tuned:	Contributing Anti-Stokes transition:
Q	P, Q, R	Q
P	O, P, Q	P & R
R	S, R, Q	P & R

The fundamental interpretation of the resonant CARS spectrum of OH therefore involves straightforward counting of resonances, and it is anticipated that the spectrum will consist of contributions from "double resonances." Detailed calculations which will be discussed later show that double resonances of the a-n, a-n' type will make little contribution, and that the primary features are accounted for by a-n, a-b double resonances. Hence, one expects the resonant CARS spectrum of OH to consist of triplets if only the vibrational fundamental (v = 0 to v =1) and no vibrational overtones ($\Delta v > 1$) are considered.

In order to perform quantitive evaluations of Eq. 2, it is necessary to have accurate spectroscopic information about vibration-rotation energy levels in the ground (X) and upper (A) electronic states, as well as values for the electronic transition dipole matrix elements. Fortunately, extensive investigations of this molecule have provided a great deal of information about these quantities. Specifically, tabulations of vibration-rotation energy levels have been published by Coxon,[14] and the absolute values of the electric dipole matrix elements can be deduced from the theoretical investigations of Chidsey and Crosley.[15] Values for the pressure-broadened linewidths also are needed, but reasonable estimates can be made here. Linewidths will be of great concern only if significant line-to-line variations are expected; at the extremely high gas temperatures of main interest in these investigations there are reasons for expecting this not to be the case. There is also a question of the proper phase to choose for the electric dipole matrix elements, because Franck-Condon factors are in general complex quantities. As Druet, et al.[8] have shown, the phase of the Franck-Condon factor is not of concern if only one vibrational level in the upper A state contributes to the anti-Stokes summation in Eq. 2. Indeed, this is the case in OH.

Using the energy level tabulations of Coxon,[14] and the Einstein A-coefficients of Chidsey and Crosley,[15] the absorption spectrum of the 1-0 A-X has been synthesized from the following expression for line intensity[16]

$$S_{v''J''}^{v'J'}(T) = \frac{1}{8\pi c\nu^2}\left(\frac{N}{p}\right)\frac{e^{-1.44E''/T}}{Q_{vR}} A_{v''J''}^{v'J'}(2J'+1)\left(1-e^{-1.44\nu/T}\right) \qquad (3)$$

where ν is the transition frequency and E" is the energy in the ground state. Because the satellite bands have been ignored, six bands (two each of P, Q, & R) contribute to the synthetic spectrum shown previously (Fig. 5). The R-bands show the expected reversal at higher values of rotational quantum number. The 1-0 system has been chosen for this calculation because our experiments have been conducted with the pump source frequency chosen to coincide with those of various lines in this system, for the reasons discussed in the section on OH spectroscopy. A high resolution predicted spectrum was illustrated above (Fig. 6).

In order to synthesize the resonant CARS spectrum of OH, electric dipole matrix elements were computed by employing the rovibrational transition probabilities of Chidsey and Crosley[15] and the rotational line strength formulas of Earls.[16] The complicated expression (Equations 1 and 2) for the third order resonant susceptibility undergoes a drastic simplification because one is concerned with only one a-n transition; the allowed Raman resonances are well separated and do not overlap; and only one or two (see (3)) anti-Stokes resonances a-n' will make contributions. If one assumes that only the lower vibrational state is significantly populated ($\rho_{bb} = \rho_{nn} = 0$), and if only one anti-Stokes resonance is important, then the resonant contribution to the third-order susceptibility (Eqn. 1) reduces to:

$$\chi_{ab}^{(3)} \simeq \frac{N\rho_{aa}^{(0)}}{\hbar^3(\omega_{ba}-\omega_1+\omega_2-i\Gamma_{ba})}\frac{\mu_{an'}\mu_{bn'}}{(\omega_{n'a}-\omega_3-i\Gamma_{n'a})} \times \frac{\mu_{an}\mu_{bn}}{(\omega_{na}-\omega_1-i\Gamma_{na})} \cdot \qquad (4)$$

A search was first undertaken for triple resonances; for each electronic transition in the 1-0 manifold, pump coincidence was assumed and the allowed Raman resonance frequencies calculated. The resulting anti-Stokes frequencies were then compared to the frequencies of the allowed transitions in the 2-0 manifold. This computer search confirmed the earlier expectation that no close triple resonances can be expected. The closest coincidence was about 4 cm^{-1} for the pump tuned to the $P_2(13)$ transition; no great enhancement is expected because the Boltzmann population factor for this transition is relatively small for the range of gas temperatures of interest.

Sample CARS calculations are presented in Figs. 8-10 for the pump tuned to various 1-0 A-X transitions. In each case, a triplet is predicted; each sharp feature in the spectrum represents a double resonance of the type a-n, a-b. The relative strengths of the features are determined by the matrix elements which occur in Eq. 2, and also by the anti-Stokes denominators in that expression. Although no triple resonance is represented here, some of the Raman resonances are associated with anti-Stokes frequencies that lie much closer to anti-Stokes resonances (in the 2-0 A-X system) than others, and are accordingly enhanced. The relatively weak features in Figs. 8-10 correspond to Raman resonances whose anti-Stokes frequencies lie relatively far from the allowed anti-Stokes resonances. The large rotational constant (B = 19 cm^{-1}) of OH gives rise to the very large separations between outer lines that are evident in Figs. 8-10. This separation decreases for lower values of J probed by the pump laser, as evident by comparing the magnitudes of the outer line separations in Figs. 9 and 10.

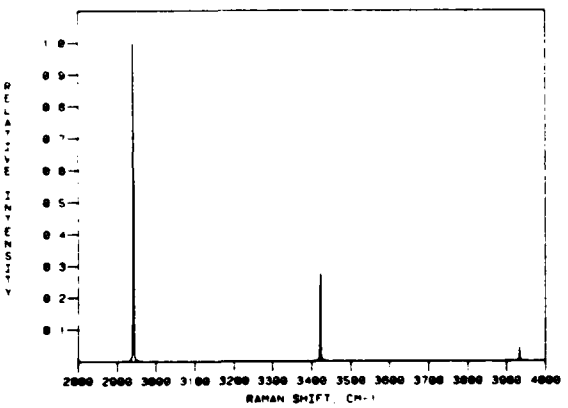

Fig. 8 Predicted resonant CARS spectrum for ω_1 resonant on Q_1 (14). T = 2500°K

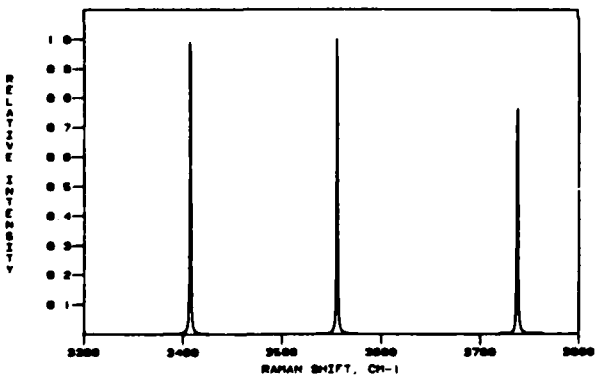

Fig. 9 Predicted resonant CARS spectrum for ω_1 tuned to $Q_1(4)$. T = 2500°K

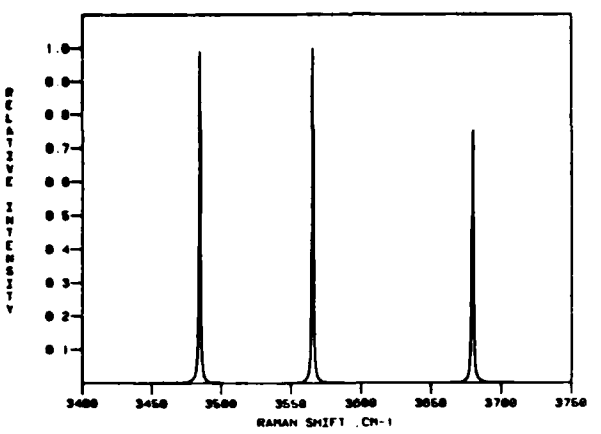

Fig. 10 Predicted resonant CARS spectrum for ω_1 tuned to $Q_1(2)$.

The interpretation of the resonant CARS spectrum of OH in terms of third-order perturbation theory thus results in the prediction of a rather simple spectrum consisting of well-separated triplets. As has been emphasized by Druet and co-workers,[8] however, the perturbation expression (1) for the third-order susceptibility will not be applicable if the pump or Stokes powers give rise to appreciable saturation. As will be seen, there is evidence of saturation in the experimental spectra obtained in these investigations, and this may preclude a simple interpretation of the experimental results. Under such conditions, corrective terms can, in principle, be applied (Druet, et al.,);[8] but a better theoretical approach might be along the lines of the analysis of strong-field effects in CARS by Wilson-Gordon, Klimovsky-Baird, and Friedmann.[17] They perform a full solution of the density matrix equation of motion for a three level system, and obtain analytical solutions in various limiting situations. Equally important is the question of collisional redistribution of population. As will be seen, although the experimental results do confirm the basic triplet structure, there is additional satellite structure around each basic component of the triplet that is suggestive of collisional transfer to adjacent rotational states. The question thus arises as to whether rotational redistribution within the upper A state and/or collisional electronic quenching to the ground X state could give rise to extra coherences. This problem may have connections with the "pressure-induced extra extra resonances" that have been predicted and observed by Prior, et al.[18] An interpretation of these extra resonances has been carried out by Grynberg,[19] who employs the formalism of the "dressed atom". These effects are areas of future investigation and are in the forefront of resonant CARS theoretical research.

Experimental

Several important factors must be carefully considered in the design of a resonant CARS experiment which attempts to detect a molecular free radical in the gas phase. The problems are compounded by the fact that the OH electronic transitions lie in the ultraviolet. The requirement of working in the UV introduces the additional complexities of frequency doubling two narrowband tunable dye lasers, working exclusively with fused silica optics, manipulating and detecting ultraviolet beams, and dealing with dichroic mirrors and filters that are only partially effective in rejection of unwanted wavelengths, which at the same time, severely attenuate the desired wavelength.

The configuration conventionally employed for resonant CARS makes use of two tunable, narrowband dye lasers whereby the ω_1 laser is tuned to a selected electronic resonance and held fixed, and then slowly scanning the Stokes laser (ω_2) which generates the resonant CARS spectrum, ω_3. The experimental configuration employed at UTRC is shown schematically in Fig. (11). The two tunable narrowband dye lasers, DL-1 and DL-2, are synchronously driven with the second harmonic (532 nm) of a Quanta-Ray pulsed neodymium YAG laser operating at 10 Hz. The partial mirror (PM) allots about 40 percent of the 532 nm radiation to a commercial pulsed dye laser (Quanta-Ray PDL-1), denoted DL-2, and the remaining portion to a homemade laser (DL-1) of the Littman grazing-grating configuration.[20] Each dye laser consists of side-pumped oscillator and preamplifier stages, followed by an end-pumped amplifier stage. Both lasers produce radiation of frequency width less than 0.1 cm^{-1} and energy per pulse between 10 and 20 millijoules, depending upon the laser dye chosen.

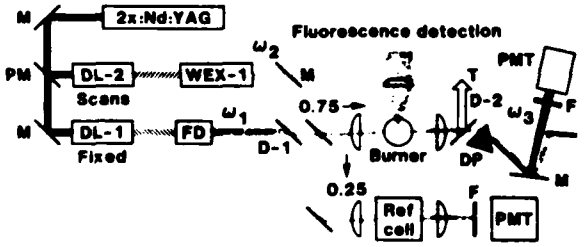

Fig. 11 Experimental arrangement for obtaining resonant CARS spectrum of OH.

As stated previously, the outputs from both dye lasers must be frequency doubled. For the ω_1 laser, frequency doubling is a trivial task and requires only a manually-adjustable second harmonic crystal, FD, in the figure. However, because ω_2 is scanned, an automatic angle-tuned device which maintains constant output power of the second harmonic frequency as the fundamental is tuned, must be employed. A WEX-1 (Quanta-Ray) performs this task over the fundamental dye laser spectrum at scan rates in excess of 0.05 nm/sec. Second harmonic conversion efficiency appears to be about 10 percent for both lasers; hence, ultraviolet energies are between 1 and 2 millijoules per pulse, which corresponds to peak powers of 100 to 200 kW.

The two ultraviolet beams are combined with a dichroic mirror and focussed into the flame in the collinear CARS configuration. The beams emerging from the flame, now containing the CARS frequency also, are recollimated and directed to the detection system. ω_1 and ω_2 are partially removed with the dichroic D-2 and trapped in the trap, T. Because the dichroic is unsuccessful in completely removing ω_1 and ω_2 from ω_3, the three beams are spatially separated with the dispersing prism, DP. The unwanted beams are masked out and ω_3 is allowed to enter a filtered photomultiplier, PMT. The reference cell leg of the experiment is derived by picking off 25 percent of the incident beams and focussing into a high pressure cell and detecting the nonresonant(non-vibrationally resonant) CARS signal. Unfortunately the reference cell leg did not function as well as anticipated, hence all the CARS spectra displayed below are uncorrected for laser power variation and dye laser profile.

A most essential feature of the experiment is the emission/fluorescence detection arm shown perpendicular to the CARS beams, above the burner, in the diagram. This portion of the experiment serves to calibrate a monochromator through the emission spectrum of OH from a methane/oxygen flame, obtained with the aid of a chopper and lock-in detector. As an example, a portion of the 1-0 emission from OH over a 50 Angstrom span is shown in Fig. (12). A few of the rotational lines are identified for illustration. More importantly, this subsystem serves to both indicate when resonance excitation is achieved and to identify the particular transition which is resonant. This is done by recording the laser-induced fluorescence by use of a boxcar integrator following the monochromator-PMT. The LIF spectrum for ω_1 exciting the $Q_1(4)$ line of the 1-0 band of OH is shown in Fig. (13). This type of spectrum, much different from the emission spectrum, clearly and uniquely identifies the resonance on

$Q_1(4)$ because of the strong fluorescence from $P_1(4)$.

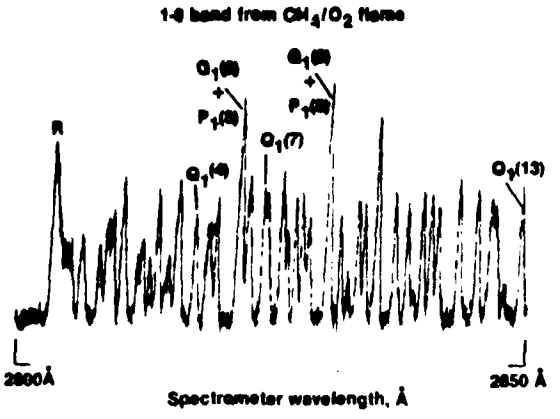

Fig. 12 OH emission spectrum used for calibration.

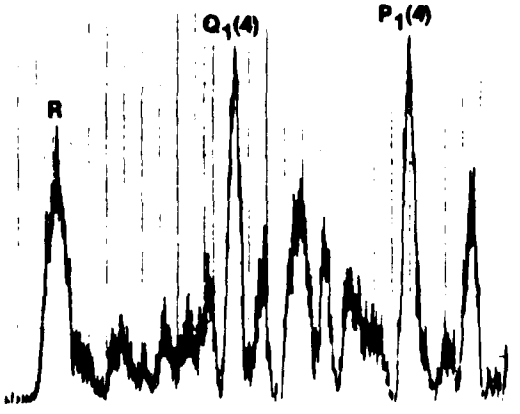

Fig. 13 Laser-induced fluorescence spectrum for ω_1 resonant on $Q_1(4)$.

The burner used throughout these studies consisted of a staggered array of stainless steel capillary tubes (0.125 in OD) which were ground flush with an edge-cooled brass plate which held the tubes in place. The matrix of alternating fuel/oxidizer tubes was surrounded by an outer layer of tubes which provided a nitrogen sheath to stabilize the flame. During the course of this investigation, a methane/oxygen flame has been used rather than the more tempermental hydrogen/oxygen flame. This type of burner produces a flame which is very uniform in appearance. The burner is mounted on a translation stage which can be moved in the vertical direction so that the CARS laser beams can be varied in height relative to the burner surface.

Resonant CARS Results

The first demonstration of resonant CARS in OH was obtained with ω_1 resonant on the $P_1(9)$ line of the 1-0 vibronic band. The spectrum is shown in Fig.(14). This type of spectrum (a scanned CARS spectrum) is obtained by scanning the ω_2 dye laser, while recording the change in intensity of the ω_3 signal falling on the detector. The region of the spectrum to the left is the water CARS spectrum which is not an electronically resonant spectrum. However, because of the great abundance of water vapor in this flame, the "normal" CARS spectrum is easily observed. The sharp rise occurring around 2591 Å is the bandhead of the water CARS spectrum. The resonant CARS of OH occurring in the tail of the water CARS spectrum, has its strongest peak at 2602 Å and represents a case where ω_1 has not been precisely tuned to the center of resonance. In contrast the resonant CARS spectrum of OH with ω_1 carefully tuned to the $Q_1(14)$ line (adjacent to the $P_1(9)$) is shown in Fig. (15). For this case, the water CARS spectrum is barely discernible, while the OH lines are much stronger, at least 5 times stronger. This is good evidence that resonant CARS is being observed, because the water concentration is at least four to five times that of OH in the CH_4/O_2 flame, and because CARS signals scale as concentration squared, the normal CARS of OH would be less than 0.1

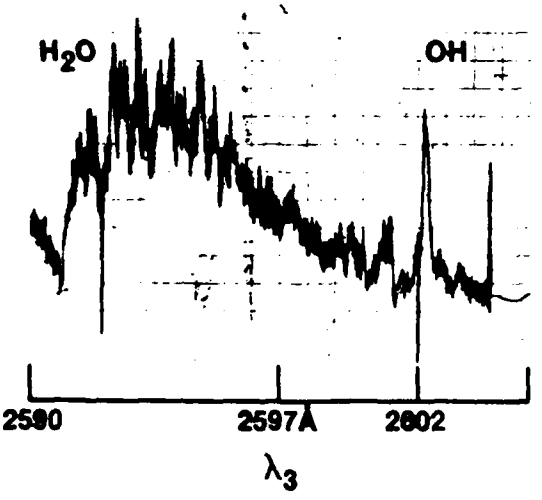

Fig. 14 Resonant CARS spectrum first obtained for ω_1 resonant on $P_1(9)$.

that of the H_2O CARS signal. In other words, it would be nearly totally lost in the water CARS band. The enhancement factor for the OH resonant CARS may even be larger than is apparent, because the true scaling of the CARS signal involves a consideration of linewidths and constructive/destructive interferences between lines.

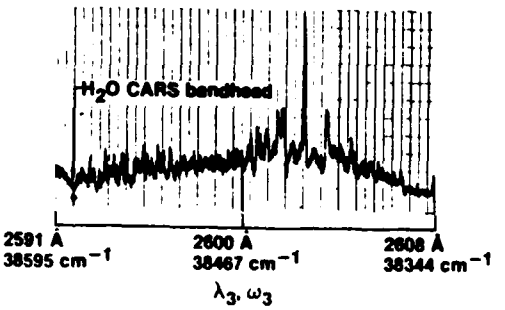

Fig. 15 Resonant CARS spectrum obtained for ω_1 tuned to $Q_1(14)$.

The resonant CARS spectra obtained for the $P_1(9)$ and $Q_1(14)$ reonances are incomplete with respect to the predicted CARS spectra of Figs (8) to (10). They are incomplete in the sense that the outermost lines are not observed in the experiment, because of the limited spectral tuning range of ω_2. The spacing between these components is 2B (2J + 1), where B is the rotational constant for OH, approximately 19 cm^{-1}. Hence, for high J values, the separation can be several hundred wavenumbers and far beyond the tuning range of a single laser dye. For these reasons, it was decided to move ω_1 toward resonances with lower J values, namely, $Q_1(4)$ and $Q_1(2)$. Examples of resonant CARS spectra for these two cases are shown in Figs. (16) and (17) respectively. As may be seen

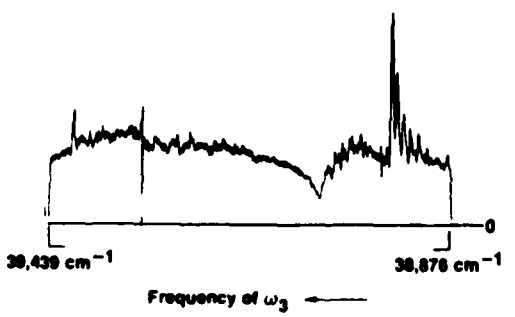

Fig. 16 Wide frequency scan of resonant CARS spectrum for resonance on $Q_1(4)$.

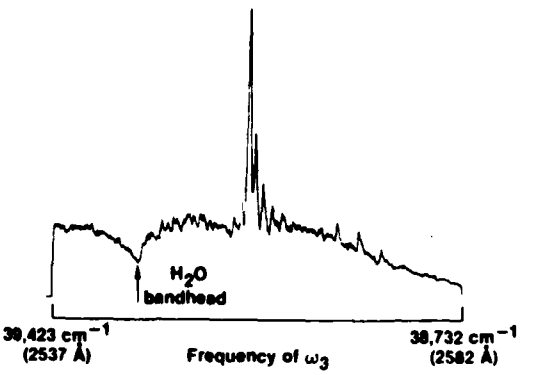

Fig. 17 Resonance CARS spectrum for ω tuned to $Q_1(2)$.

the scans cover a reasonably wide frequency range, in excess of 300 cm^{-1}. For the case of the $Q_1(4)$ spectrum, considerable structure may be seen to the left of the water CARS bandhead. These lines have not yet been identified as positively originating from OH, however. For the $Q_1(2)$ resonance CARS, some structure is observed to the right of the strong central OH resonant CARS band, at approximately the proper spacing. This structure does not consist of a single line, but also exhibits some satellite lines, contrary to theoretical prediction.

A preliminary exploration of saturation was made by reducing the intensity of the ω_1 beam with fused silica flats and partially reflecting UV mirrors. The maximum attenuation so obtained was a factor of 5.5. In order to obtain a reasonable signal strength at this level of attenuation, the PMT supply voltage was increased. The results of this test are shown in Fig. (18). Note that there is a

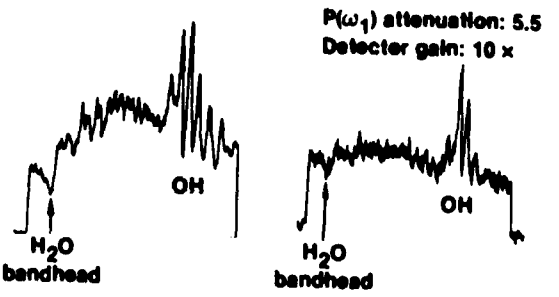

Fig. 18 Change in the resonant CARS spectrum with attenuation of ω_1 intensity.

considerable change in the shape of the OH spectrum and in the number of lines. Note also that the water CARS spectrum is barely discernible in the attenuated ω_1 spectrum. The increased gain required to maintain the same signal level was approximately 10; because the CARS signal scales as the square of the ω_1 power, a reduction of about 30 should have been seen. This observation, along with the change in shape is evidence that saturation must be considered. A more thorough study is called for; one which also includes attenuation of the ω_2 laser beam to determine if both laser beams can contribute to saturation of the resonant CARS process.

Finally, an initial study of the sensitivity of the resonant CARS spectrum to changes in concentration was performed by changing the height of the incident CARS laser beams relative to the height of the burner surface. The results are shown in Fig. 19. where spectra for 0.5

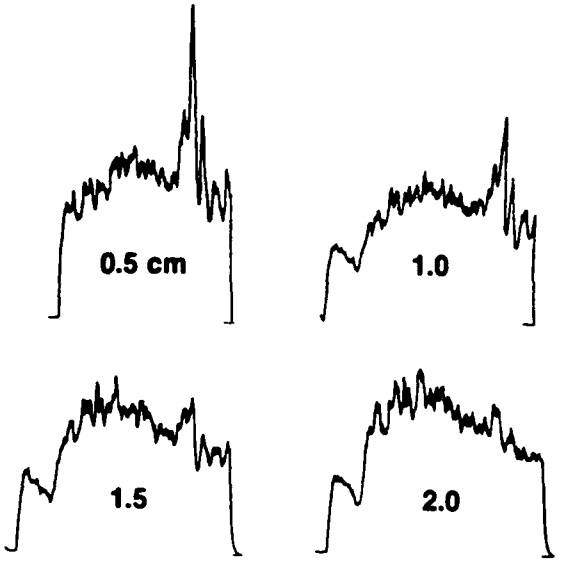

Fig. 19 Variation of the resonant CARS spectrum with change in laser beam height relative to burner surface.

cm increments are displayed. The scans shown cover just the spectral region of the water and OH CARS bands. Clearly, the OH concentration decreases as the CARS beams are moved away from the burner surface; at the same time, the water concentration appears to be increasing slowly. At the largest separation, 2 cm , there is still some indication of OH, as a modulation on the background. Future studies will involve a detailed calibration of the concentrations of both OH and water throughout the flame, as well as the temperature distribution, so that resonant CARS as a quantitative diagnostic may be properly assessed. Saturation may prove to be a problem for quantitative measurements; however even in the case of saturation, it may be possible to construct a working curve of concentration vs. signal strength.

Conclusions

Electronically resonant CARS of the OH radical has been demonstrated in a very hot methane/oxygen flame. The resonant CARS spectrum was generated by use of two frequency-doubled, pulsed, narrowband dye lasers, one of which was tuned and then fixed on a selected OH X-A transition, while the other other was scanned over the appropriate range. The OH resonant CARS signal is strong compared to the water CARS spectrum, even though water is much more abundant than OH in the flame. Resonant CARS was observed for several different electronic resonances and was quite sensitive to precise tuning. The theory of resonant CARS in the OH radical has been treated and the predicted appearance of OH resonant CARS spectra presented. Saturation, for which there is some experimental evidence, has not been included in the theory yet. Agreement between theory and experiment is good, except for the experimental observation of satellite structure about the central line, probably caused by collisional redistribution of population in rotational energy levels. The variation of the resonant CARS spectrum as a function of laser beam height in the flame was observed and offers promise that resonant CARS may be applicable to quantitative measurements. Future studies will involve refinement of the theory to include saturation, further experimental work to assess the feasibility of making quantitative measurements in a flame, a thorough exploration of saturation effects, measurement of the resonance enhancement factor, and precise spectral line positions. Another interesting possibility which must be explored is that of pressure-induced extra resonances in four-wave mixing processes such as CARS, a so-called PIER-4 process.[18] Additionally, triple resonances will be searched for, if a theoretical survey suggests that there are promising possibilities.

Acknowledgements

The authors wish to acknowledge valuable discussions with Prof. Nicolaas Bloembergen of the Harvard University Physics Department and with Dr. D. R. Crosley of SRI International. Thanks are also due Edward Dzwonkowski and Normand Gantick for assistance with the experiments.

References

1. Eckbreth, A.C., and R.J. Hall, "CARS Thermometry in a Sooting Flame," Combust. Flame, Vol. 36, 1979, pp. 87-98.

2. Pealat, M., J-P.E. Taran, J. Taillet, M. Bacal, and A.M. Bacal, and A.M. Brunetau, "Measurement of Vibrational Populations in Low-pressure Hydrogen Plasma by Coherent Anti-Stokes Raman Scattering," J. Appl. Phys., Vol. 53, 1981, pp. 2687-2691.

3. Stenhouse, I.A., D.R. Williams, J.B. Cole, and M.D. Swords, "CARS in an Internal Combustion Engine," Vol. 1977, pp. 3819-3825.

4. Eckbreth, A.C., G.M. Dobbs, J.H. Stufflebeam, and P.A. Tellex, " CARS Temperature and Species Measurements in Augmented Jet Engine Exhausts," AIAA Paper No. 83-1294. To be presented at the AIAA/ASME/SAE 19th Joint Propulsion Conference, Seattle, Washington, June 27-29, 1983.

5. Druet, S., and J-P.E. Taran, "Coherent Anti-Stokes Raman Spectroscopy," in Chemical and Biological Applications of Lasers, C.B. Moore, Ed., Academic Press, New York, 1979, pp. 187-172.

6. Tolles, W.M., J.W. Nibler, J.R. McDonald, and A.B. Harvey, "A Review of the Theory and Application of Coherent Anti-Stokes Raman Spectroscopy (CARS)," Appl. Spect., Vol. 32, 1977, pp. 253-272.

7. Verdieck, J.F., J.A. Shirley, R.J. Hall, and A.C. Eckbreth, "CARS Thermometry in Reacting Systems," in Temperature, Its Measurement and Control in Science and Industry, American Institute of Physics, New York, 1982, pp. 595-608.

8. Druet, S.A.J., B. Attal, T.K. Gustafson, and J-P.E. Taran, "Electronic Resonance Enhancement of Coherent Anti-Stokes Raman Scattering," Phys. Rev. A., Vol. 18, 1978, pp. 1529-1557.

9. Guthals, D.M., K.P. Gross, and J.W. Nibler, "Resonant CARS Spectra of NO_2," J. Chem. Phys., Vol. 70, 1979, pp. 2393-2398.

10. Attal, B., D.Debarre, K. Muller-Dethlefs, and J-P.E. Taran, "Resonance-Enhanced Coherent Anti-Stokes Raman Scattering in C_2," To be published in J. de Phys. (Paris). 1983.

11. Crosley, D.R., "Collisional Effects on Laser-Induced Fluorescence Flame Measurements," Opt. Eng., Vol. 20, 1981, pp. 511-521.

12. Dieke, G.H., and H.M. Crosswhite, "The Ultraviolet Bands of OH," J. Quant. Spectrosc. Radiat. Transfer, Vol. 2, pp. 97-199.

13. Bloembergen, N., H.L. Lotem, and R.T. Lynch, "Lineshapes in Coherent Resonant Raman Scattering," Indian J. Pure and Appl. Phys., Vol. 16, 1978, pp. 151-158.

14. Coxon, J.A., "Optimum Molecular Constants and Term Values for the X and A States of OH," Can. J. Phys., Vol. 58, 1980, pp. 933-949.

15. Chidsey, I.L., and D.R. Crosley, "Calculated Rotational Transition Probabilities for the A-X System of OH," J. Quant. Spectrosc. Radiat. Transfer, Vol. 23, 1980, pp. 187-199.

16. Earls, L.T., " Intensities in $^2\Pi$ - $^2\Sigma$ Transitions in Diatomic Molecules," Phys. Rev., Vol. 48, 1935, pp. 423-424.

17. Wilson-Gordon, A.D., R. Klimovsky-Baird, and H. Friedmann, "Saturation Effects in Coherent Anti-Stokes Raman Scattering," Phys. Rev. A., Vol. 25, 1982, pp. 1580-1595.

18. Prior, Y., A.R. Bogdan, M.W. Dagenais and N. Bloembergen, "Pressure-Induced Extra Resonances in Four-Wave Mixing," Phys. Rev. Lett., Vol. 46, 1981, pp. 111-114.

19. Grynberg. G., "Resonances Between Unpopulated Levels in Non-Linear Optics," J. Phys. D., Vol. 14, 1981, pp. 2089-2097.

20. Littman, M.G., and H.J. Metcalf, "Spectrally Narrow Pulsed Dye Laser Without Beam Expander," Appl. Opt., Vol. 17, 1978, pp. 2224-2227.

Electronically Resonant CARS Detection of OH

J.F. Verdieck, R.J. Hall, and A.C. Eckbreth

Reprinted from **Combustion Diagnostics by Nonintrusive Methods**, *edited by Jeffrey A. Roux and T. Dwayne McCay, Vol 92 of Progress in Astronautics and Aeronautics, 1984.*

Electronically Resonant CARS Detection of OH

James F. Verdieck,* Robert J. Hall,* and Alan C. Eckbreth*
United Technologies Research Center, East Hartford, Connecticut

Abstract

CARS (coherent anti-Stokes Raman spectroscopy) is a nonlinear spectroscopic technique capable of making remote, highly accurate measurements of temperature and concentration which are both temporally and spatially precise, in extremely difficult environments such as internal combustion engines and gas turbine exhausts. A major disadvantage of CARS methods is that application is limited to those species whose concentration is 1 % or greater. In order to extend CARS detectivity, electronically resonantly enhanced CARS can be employed, whereby one of the CARS laser frequencies is selected to be resonant with an electronic transition. This results in a large signal enhancement (possibly several orders of magnitude). This paper reports the results of applying resonant CARS to the detection of the hydroxyl radical in a methane/oxygen flame. Both the theory of electronically resonant CARS, predicted spectra, and the experimental procedure are described in detail. The variation of the resonant CARS spectra with different choices of electronic resonance is shown. A preliminary demonstration of saturation is also illustrated, as is the correlation of the resonant CARS spectrum with dependence of OH concentration on flame height.

Introduction

CARS (coherent anti-Stokes Raman spectroscopy) is a nonlinear optical process wherein three optical fields are combined in a material medium to generate a fourth optical field. As conventionally employed, two laser frequencies,

Presented as Paper 83-1477 at the AIAA Thermophysics Conference, Montreal, Canada, June 1-3, 1983. Released to AIAA to publish in all forms.

*Senior Research Scientist, Applied Laser Spectroscopy Laboratory.

ω_1(the pump beam) and ω_2(the Stokes beam), are mixed to produce the CARS frequency, ω_3, which appears as a coherent, collimated beam. This is illustrated in Fig. 1a. The CARS signal is large and easily detected (even in the prescence of particles or a highly luminous background) when the frequency difference between the two input frequencies corresponds to a Raman-active molecular vibration or rotation (or an electronic transition). Because CARS is a coherent, nonlinear process, laser beams are required to provide the proper phases of the optical fields in time and space, and the high intensity to enhance the nonlinear aspect of the process. Usually, high-peak power pulsed lasers are employed to generate CARS, particularly for combustion diagnostic applications. Photon energy is conserved in the CARS process (in contrast to the Raman effect), as illustrated in Fig. 1b. Note that $\omega_1 > \omega_2$. Fig. 1c exhibits two distinct methods of generating a CARS spectrum. One of these methods is to employ a broadband (100 cm^{-1} wide) Stokes laser, which results in the generation of the entire CARS spectrum of interest from each laser shot. This particular method is very useful for combustion diagnostics because single-shot (typically 10 nsec) thermometry can be performed. The second method uses two narrowband laser and tunes one of these, generating the CARS spectrum by scanning. It is this second, scanned technique which is utilized to generate resonantly enchanced CARS, by scanning ω_2 while holding ω_1 fixed on an electronic transition.

CARS applications are diverse and too numerous to catalog in detail here. It is an important spectroscopic technique well-suited for fundamental studies of molecules,

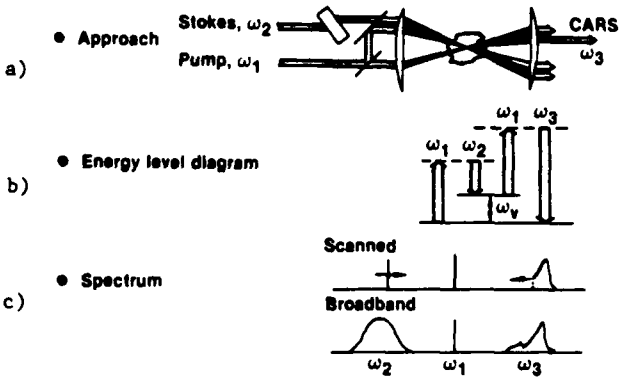

Fig. 1 Schematic diagram illustrating the basic concepts of CARS spectroscopy.

large and small. CARS has been repeatedly demonstrated to be a superior technique for remote diagnostics for combustion research, on both a laboratory scale and for large-scale practical devices. Examples include CARS temperature and concentration measurements in sooty flames,[1] plasmas,[2] internal combustion engines,[3] and gas turbine engines.[4] The theory and application of CARS have been extensively reviewed; these reviews may be consulted for detailed descriptions.[5-7]

A major disadvantage of CARS diagnostics methods is that, at atmospheric pressure, they are limited in application to species whose concentration is about 1 % or greater. A means of overcoming this limitation is to enhance the CARS signal through electronic resonance. Recall that the normal CARS process is vibrationally resonant; if in addition, one of the input CARS frequencies is resonant with an electronic transition, a large increase in the CARS signal occurs. This increase can be a factor of several hundred over the normal CARS effect. Electronically-resonant CARS (resonant CARS for short) has been observed for several large molecules in solution phase; however, to date, only a limited number of molecules have been observed to exhibit resonant CARS in the gaseous phase, namely I_2[8], NO_2[9], and most recently, C_2[10]. The reason for this limited application in gas phase is clear; there are very few simple, small molecules which absorb visible light(where dye lasers work efficiently). Indeed,the last cited case, C_2, is a radical which must be generated in a flame or a microwave discharge.[10]

The hydroxyl radical was chosen for study at this laboratory because of its ubiquitous presence and extreme importance in combustion chemistry. OH enters into the oxidation mechanisms of nearly all hydrogen-containing fuels, and plays an essential role in the combustion reaction pathways of most types of hydrocarbons. Hydroxyl radical reactions are usually very rapid (because OH is a radical, activation energies are small) and OH often enters into explosive chain reactions. OH is also important in atmospheric chemistry and has been implicated in acid rain formation from nitrogen and sulfur oxides. For these important reasons, it is important to be able to detect and measure the concentration of the OH radical in difficult environments.

Optical methods presently employed to measure OH concentrations are UV absorption spectroscopy and laser-induced fluorescence spectroscopy (LIFS). The absorption method is readily applied and useful where spatial resolution is not required. Even where applicable, gradient and

edge effects can degrade absorption measurement accuracy. LIFS is a point measurement technique which enjoys good success in carefully controlled laboratory devices operating cleanly at low pressure.[11] However, in practical combustion environments, fluorescence methods can suffer from interferences, such as fluorescence from other species and from laser-induced particle incandescence. The major problem with fluorescence techniques is collisional quenching, particularly for application in high pressure devices. In contrast, CARS diagnostic measurements have been demonstrated in several practical combustion systems such as highly luminous sooting flames, internal combustion engines, gas turbine combustors, solid propellant flames, and alumina particle laden flows. The principal reason for the success of CARS in these very difficult combustion systems is the fact that the CARS signal emerges as a coherent beam, all of which can be captured. This provides a unique advantage over incoherent techniques, such as fluorescence, particularly when the optical access is limited. Because CARS methods have proven superior in these types of environment, it is essential to extend the sensitivity for CARS to radicals such as OH.

In the sections which follow, the progress on application of resonant CARS to the detection of OH is described. The effort at UTRC has been and continues to be a combined theoretical and experimental program. The first section is a basic primer on OH spectroscopy, required for application of resonant CARS. Following this section is a presentation of the theory of resonant CARS with predicted resonant CARS spectra for comparison with experimental spectra. Issues of saturation and rotational state redistribution are not considered because they are so difficult to model. A description of the experimental apparatus employed follows the theoretical section. The results of the experiments to date, are presented mainly through display of the resonant CARS spectra obtained from different ω_1 electronic resonances, variation of incident laser power, and changing the laser beam height relative to the burner surface. Conclusions reached from these investigations, and plans for future studies are given in the final section.

Spectroscopy of the Hydroxyl Radical

It is essential to understand the electronic, vibrational, and rotational aspects of OH spectrosopy in order to wisely select the resonant CARS pump laser frequency, ω_1. Once ω_1 has been chosen, the Stokes frequency, ω_2, is determined by the OH vibrational shift. The

spectral positions of the excitation frequencies, although a matter of some choice, depends strongly on the laser dyes available which yield high second-harmonic conversion efficiency in the appropriate region of the ultraviolet.

The spectroscopy of the OH radical is rather complicated for a diatomic molecule. This complexity arises mainly from the unpaired electron spin and the non-zero orbital angular momentum of the electronic ground state. Without going into fine detail, the result of spin-orbit coupling is a $^2\Pi$ electronic ground state which is split by ca. 126 cm^{-1}. This $^2\Pi$ state is inverted with the $\Omega = 3/2$ state lying below the 1/2 state. Following Dieke and Crosswhite,[12] these states are designated F_1 and F_2 respectively, and are shown, along with the first excited state, $^2\Sigma$, in Fig. 2. The splitting between the upper state components f_1 and f_2 is exaggerated to illustrate the strongly vs weakly allowed transitions from the ground electronic state (generic label, X) to the first excited state(A). Also shown in this figure are the vibrational and rotational transitions from X to A. There are no vibrational selection rules for electronic transitions, but the Franck-Condon principle governs the strength of the vibronic transitions as the middle figure indicates. Note that the convention on labeling states is v′ for the upper state and v" for the lower. Moreover, a particular transition is designated as v′,v"; hence, the 1-0 vibronic transition implies a transition, in either absorption or emission, between v′ = 1 of the A state and v" = 0 of the X state. For the case of a $^2\Pi$ state the rotational selection rule permits $\Delta J = 0, \pm 1$; therefore Q, P and R rotational branches are oberved as shown in Fig. 2. Note also that the quantum number J for this case is the total angular momentum; i.e., the sum of the orbital angular momen-

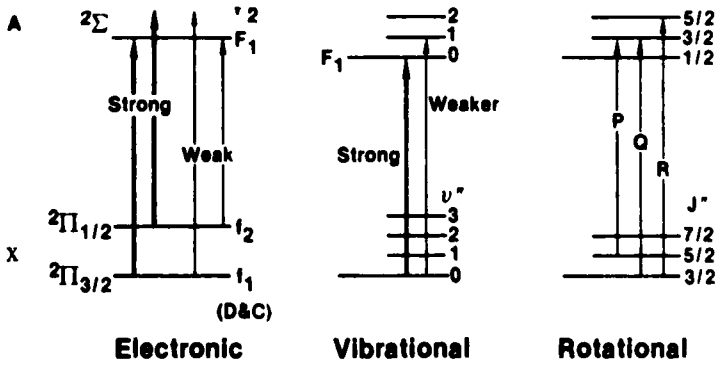

Fig. 2 Fundamental spectroscopic considerations for the OH radical.

tum, Ω, and the mechanical angular momentum of the molecule, N. For this reason, J" is half-integral and has an initial value of 3/2.

If one excludes the rotational fine structure and examines only the vibronic structure of the X to A transition of OH, a plot of vibronic bandheads results, as shown in Fig. 3. This spectrum is extremely important because, in conjunction with Fig. 4, the relative output of conventional laser dyes, it was used to determine the optimum vibronic band for the resonant CARS pump frequency, ω_1. The choice of the 1-0 band was made because it places ω_1 in the region of the very efficient laser dye, rhodamine 590, so that reasonable second harmonic power can be obtained. The Stokes frequency, ω_2, is required to lie in the range 3000-3500 cm^{-1} to the low frequency side (high wavelength) of ω_1. According to Fig. 4, the laser dye DCM covers the required range nicely, with good energy conversion. It must be noted that the 0-0 band, at 307 nm, much exploited for laser induced fluorescence, appears to be a poor choice for ω_1 because both of the laser frequencies would lie on the opposite edges of the DCM curve and the second harmonic power would be quite low.

The complete rotational structure of the 0-0 and 1-0 bands is shown in Fig. 5. This is the superposition of the P, Q, and R branches arising from both components of the $^2\Pi$ electronic ground state. In order to distinguish these components a subscript 1 or 2 is used for transitions from or to the F_1 or F_2 states, respectively. This notation is illustrated in the next figure, Fig. 6, which shows a portion of the 1-0 band greatly expanded. It is noted that there is considerable spacing--5 to 10 cm^{-1}--between lines such as $Q_1(14)$ and $P_1(9)$ in this region. A single transition is easily selected because the frequency bandwidth of the dye laser is less than 0.3 cm^{-1}.

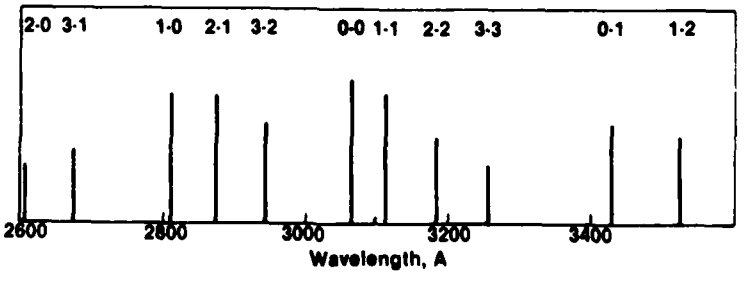

Fig. 3 Vibronic bandheads for the A to X transition of OH. Acetylene/oxygen flame at 3000 K. Adapted from Dieke and Crosswhite, Ref. 12.

In this region of the spectrum, 10 cm^{-1} corresponds to about 0.1 nm. The two transitions mentioned were employed for the first observation of resonance CARS in OH.

Resonant CARS Theory

The traditional approach to interpretation of resonance CARS spectra has been to employ the general, 48 term expression for the third-order electric susceptibility that has been derived by several authors.[8,13] This expression has been obtained either algebraically, using a perturbation expansion solution of the density matrix equation of motion, or diagrammatically, using "doubled" Feynman diagrams.

Both approaches yield equivalent results. The complete expression, showing all terms, has been presented by Bloembergen, Lotem, & Lynch.[13] Certain of the terms contain vibrationally resonant denominators which cause them to be large when the frequency difference between the Pump and Stokes sources encroaches upon Raman-active vibrational modes. If all other terms are lumped into the nonresonant background susceptibility, χ_{NR}, then the third-order electric susceptibilty may be expressed as a sum of this nonresonant term and a vibrationally resonant term which is a summation of contributions from all Raman-active modes. That is (Druet, et al.),[8]

$$\chi^{(3)}(\omega_3) = \chi_{NR} + \sum_{a,b} \chi_R^{ba} \qquad (1)$$

where a and b represent the initial and final vibration-rotation quantum numbers of a particular Raman transition whose contribution to the resonant part of the susceptibi-

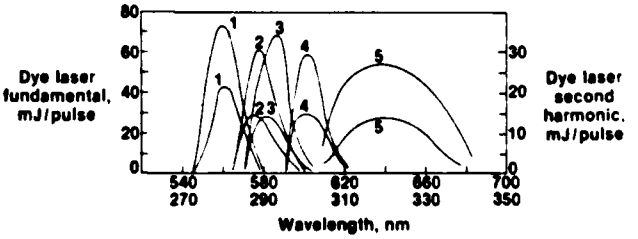

Fig. 4 Second harmonic conversion of some typical laser dyes using a 532 nm pump laser with 200 mJ/pulse. The dyes shown are: 1, Exciton R590; 2, Exciton R610; 3, Exciton Kiton Red; 4, Exciton 640; 5, Exciton DCM. Source, Quanta-Ray, Inc.

lity can be expressed as

$$\chi^{(3)}_{ab} = \frac{N}{\hbar^3}\frac{1}{(\omega_{ba}-\omega_1+\omega_2-i\Gamma_{ba})}\sum_{n'}\left(\frac{\mu_{an'}\mu_{n'b}}{\omega_{n'a}-\omega_3-i\Gamma_{n'a}}+\frac{\mu_{an'}\mu_{n'b}}{\omega_{n'b}+\omega_3+i\Gamma_{n'b}}\right)$$

$$\times\left[\sum_n(\rho^{(0)}_{aa}-\rho^{(0)}_{nn})\left(\frac{\mu_{bn}\mu_{na}}{\omega_{na}+\omega_2-i\Gamma_{na}}+\frac{\mu_{bn}\mu_{na}}{\omega_{na}-\omega_1-i\Gamma_{na}}\right)\right.$$

$$\left.-\sum_n(\rho^{(0)}_{bb}-\rho^{(0)}_{nn})\left(\frac{\mu_{bn}\mu_{na}}{\omega_{nb}-\omega_2+i\Gamma_{nb}}+\frac{\mu_{bn}\mu_{na}}{\omega_{nb}+\omega_1+i\Gamma_{nb}}\right)\right] \qquad (2)$$

In Eq. 2, N represents the OH number density, ω denotes frequency; Γ denotes pressure-broadened linewidth; ρ, Boltzmann population; and μ, electric dipole matrix element. n and n′ represent excited electronic states of the molecule, and it is apparent from examination of the denominators in Eq. 2 that electronic resonant enhancement will occur if either ω_1, ω_2, or ω_3 coincides with an allowed electronic transition. It is also apparent that selecting the pump frequency resonant with a particular a-n electronic transition "picks out" a particular initial ground vibration-rotation state a, making it possible to

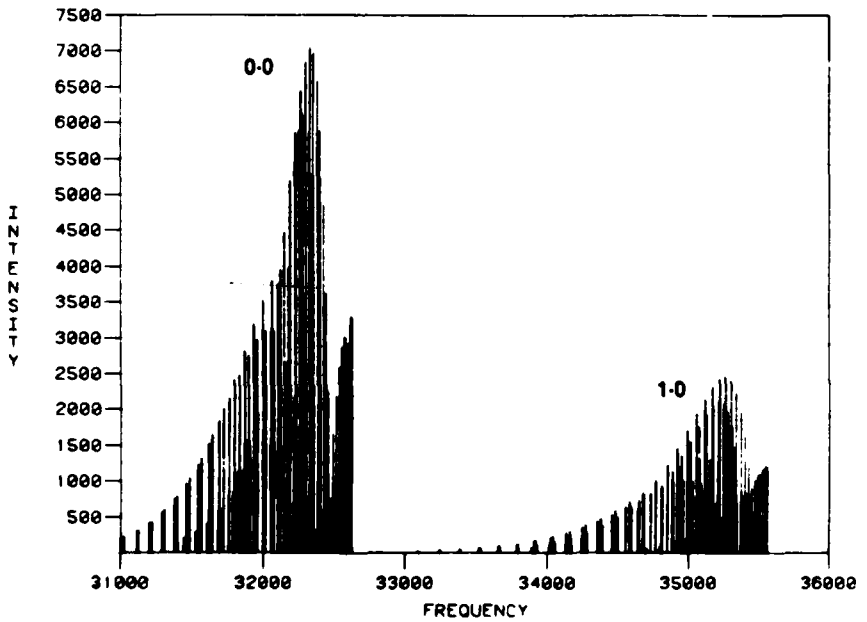

Fig. 5 Theoretical "stick" spectra of the 0-0 and 1-0 bands of the A-X transition in OH.

ignore the contributions of all other initial Raman states in the ground electronic vibrational manifold. Because the term which contains the denominator resonant in ω_2 is proportional to the population ρ_{bb} of the upper state in the Raman transition, it is reasonable to expect that its contribution will be small, particularly for a molecule like OH with a very large vibrational spacing. The rules for interpretation of resonant CARS spectra in terms of Eq. 2 have been discussed at length in the literature, with successful application to I_2,[8] N_2O,[9] and C_2[10].

One notes that if the pump frequency is made to coincide with the frequency of a particular electronic transition a-n, and the Stokes frequency is tuned to sweep out the range of Raman frequencies, there will be double resonances which occur when $\omega_1 - \omega_2 = \omega_{ab}$, or $\omega_3 = \omega_{an'}$, and the possibility of triple resonances when $\omega_1 = \omega_{an}$, $\omega_1 - \omega_2 = \omega_{ab}$, and $\omega_3 = \omega_{an'}$. The criterion for the occurrence of a triple resonance is that the transitions a-n and a-n′ be optically allowed and that $\omega_{ab} = \omega_{nn'}$. While the triple resonances do occur in molecules like I_2 and C_2 with closely spaced vibration-rotation states, they are expected to be extremely improbable in a molecule like OH with very large spacing between levels. If two distinct pump sources with slightly different frequencies are employed, then a triple

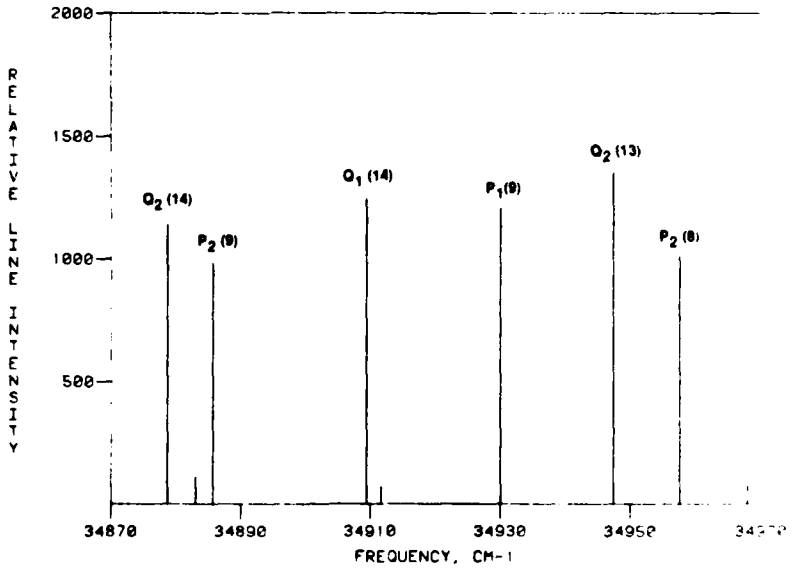

Fig. 6 High resolution "stick" spectrum of OH expanded about the $P_1(9)$ line of the 1-0 band.

resonance can be achieved in OH, but in general they should not be expected.

The electronic and vibrational spectroscopy of OH has been discussed previously. In the electronic absorption or emission spectrum, P, Q, and R branches are allowed, making possible 12 branches. However, the six satellite branches in which the F_1 or F_2 designation changes will be relatively weak, leaving six main branches. In OH vibrational spectroscopy O, P, Q, R, and S transitions are allowed. The weakness of the satellite branches in the electronic spectrum means that vibrational transitions in which the F_1 or F_2 designation changes can also be ignored. By examination of Eq. 2, and considering the selection rules for electronic and rotational transitions which must be obeyed for the resonant CARS process, it is possible to specify the types of resonances which will give rise to the spectral features in electronically resonantly enhanced OH CARS. As an example, if ω_1 is tuned to a Q-branch transition, then P, Q, and R Raman resonances will be observed, and the anti-Stokes term will be contributed by a Q-transition. This is illustrated in Fig.7. The general rules are illustrated in Table 1.

The fundamental interpretation of the resonant CARS spectrum of OH therefore involves straightforward counting of resonances, and it is anticipated that the spectrum will consist of contributions from "double resonances". Detailed calculations which will be discussed later show that double resonances of the a-n, a-n′ type will make little contribution, and that the primary features are accounted for by a-n, a-b double resonances. Hence, one expects the resonant CARS spectrum of OH to consist of triplets if only the vibrational fundamental (v=0 to v=1) and no vibrational overtones ($\Delta v > 1$) are considered.

In order to perform quantitive evaluations of Eq. 2, it is necessary to have accurate spectroscopic information

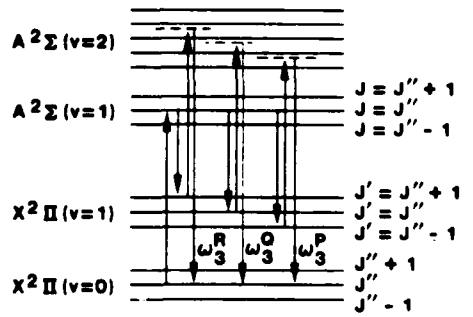

Fig. 7 Energy level diagram showing the origin of the triplet structure of the resonant CARS spectrum.

about vibration-rotation energy levels in the ground (X) and upper (A) electronic states, as well as values for the electronic transition dipole matrix elements. Fortunately, extensive investigations of this molecule have provided a great deal of information about these quantities. Specifically, tabulations of vibration-rotation energy levels have been published by Coxon,[14] and the absolute values of the electric dipole matrix elements can be deduced from the theoretical investigations of Chidsey and Crosley.[15] Values for the pressure-broadened linewidths also are needed, but reasonable estimates can be made here. Linewidths will be of great concern only if significant line-to-line variations are expected; at the extremely high gas temperatures of main interest in these investigations there are reasons for expecting this not to be the case. There is also a question of the proper phase to choose for the electric dipole matrix elements, because Franck-Condon factors are in general complex quantities. As Druet, et al.[8], have shown, the phase of the Franck-Condon factor is not of concern, if only one vibrational state in the upper A state contributes to the anti-Stokes summation in Eq. 2. Indeed, this is the case in OH.

Using the energy level tabulations of Coxon,[14] and the Einstein A-coefficients of Chidsey and Crosley,[15] the absorption spectrum of the 1-0 A-X system has been synthesized from the following expression for line intensity[16]

$$S_{v''J''}^{v'J'}(T) = \frac{1}{8\pi c\nu^2}\left(\frac{N}{p}\right)\frac{e^{-1.44E''/T}}{Q_{VR}} A_{v''J''}^{v'J'}(2J'+1)\left(1-e^{-1.44\nu/T}\right) \quad (3)$$

where ν is the transition frequency and E" is the energy in the ground state. Because the satellite bands have been ignored, six bands (two each of P, Q,and R) contribute to the synthetic spectrum shown previously (Fig. 5). The R-bands show the expected reversal at higher values of rotational quantum number. The 1-0 system has been chosen for this calculation because our experiments have been conducted with the pump source frequency chosen to coincide with those of various lines in this system, for the reasons discussed in the section on OH spectroscopy. A high resolution predicted spectrum was illustrated above (Fig. 6).

In order to synthesize the resonant CARS spectrum of OH, electric dipole matrix elements were computed by employing the rovibrational transition probabilities of Chidsey and Crosley,[15] and the rotational line strength formulas of Earls.[16] The complicated expression (Eqs. 1

and 2) for the third order resonant susceptibility undergoes a drastic simplification because one is concerned with only one a-n transition; the allowed Raman resonances are well separated and do not overlap; and only one or two (see (3)) anti-Stokes resonances a-n′ will make contributions. If one assumes that only the lower vibrational state is significantly populated ($\rho_{bb} = \rho_{nn} = 0$), and if only one anti-Stokes resonance is important, then the resonant contribution to the third-order susceptibilty (Eq. 1) reduces to

$$\chi^{(3)}_{ab} \simeq \frac{N\rho^{(0)}_{aa}}{\hbar^3(\omega_{ba} - \omega_1 + \omega_2 - i\Gamma_{ba})} \frac{\mu_{an'}\mu_{bn'}}{(\omega_{n'a} - \omega_3 - i\Gamma_{n'a})} \times \frac{\mu_{an}\mu_{bn}}{(\omega_{na} - \omega_1 - i\Gamma_{na})} \qquad (4)$$

A search was first undertaken for triple resonances; for each electronic transition in the 1-0 manifold, pump coincidence was assumed and the allowed Raman resonance

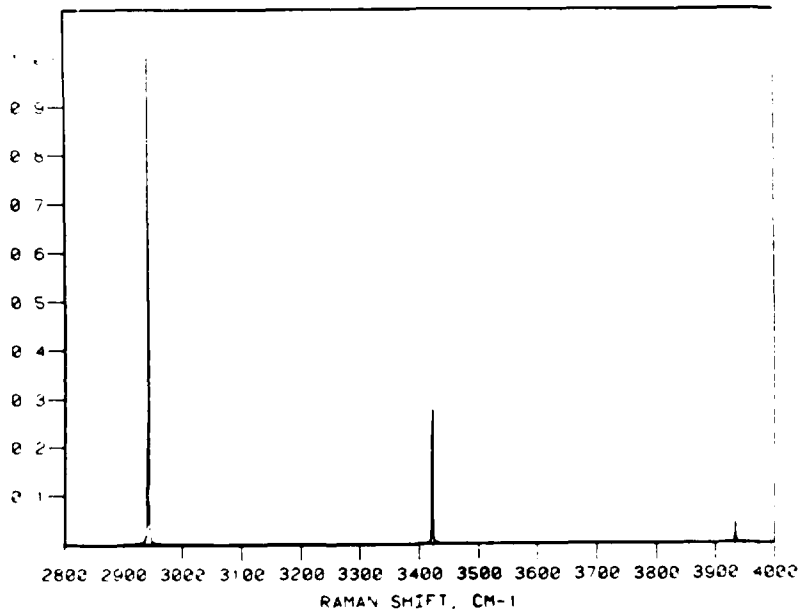

Fig. 8 Predicted resonant CARS spectrum for ω_1 tuned to $P_1(9)$.

frequencies calculated. The resulting anti-Stokes frequencies were then compared to the frequencies of the allowed transitions in the 2-0 manifold. This computer search confirmed the earlier expectation that no close triple resonances can be expected. The closest coincidence was about 4 cm^{-1} for the pump tuned to the $P_1(13)$ transition; no great enhancement is expected because the Boltzmann population factor for this transition is relatively small for the range of gas temperatures of interest.

Sample CARS calculations are presented in Figs. 8 and 9 for the pump tuned to various 1-0 A-X transitions. In

Table 1 Allowed resonant CARS transitions

Pump tuned to	Allowed Raman resonances as Stokes is tuned	Contributing anti-Stokes transition
Q	P,Q,R	Q
P	O,P,Q	P,R
R	Q,R,S	P,R

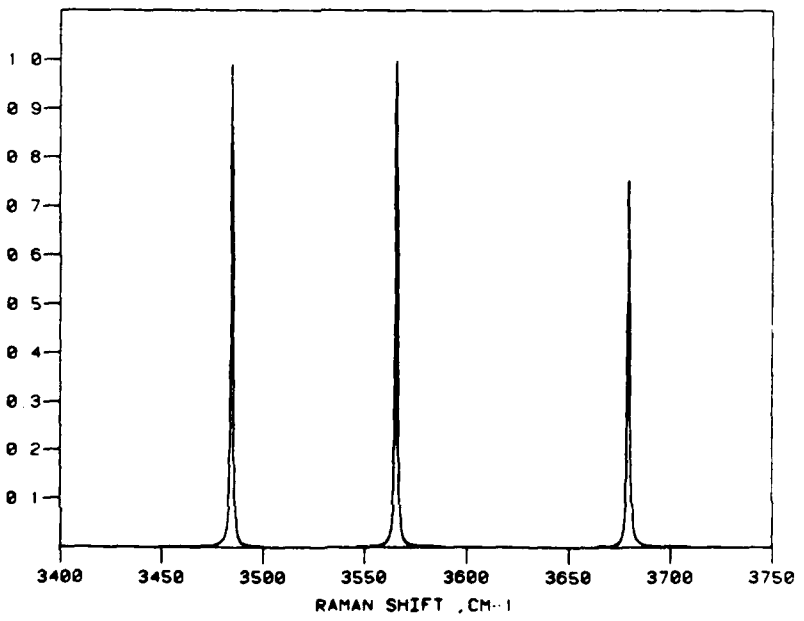

Fig. 9 Predicted resonant CARS spectrum for ω_1 tuned to $Q_1(2)$.

each case, a triplet is predicted; each sharp feature in the spectrum represents a double resonance of the type a-n, a-b. The relative strengths of the features are determined by the matrix elements which occur in Eq. 2, and also by the anti-Stokes denominators in that expression. Although no triple resonance is represented here, some of the Raman resonances are associated with anti-Stokes frequencies that lie much closer to anti-Stokes resonances (in the 2-0 A-X system) than others, and are accordingly enhanced. The relatively weak features in Figs. 8 and 9 correspond to Raman resonances whose anti-Stokes frequencies lie relatively far from the allowed anti-Stokes resonances. The large rotational constant (B = 19 cm^{-1}) of OH gives rise to the very large separations between outer lines that are evident in Figs. 8 and 9. This separation decreases for lower values of J probed by the pump laser, as evident by comparing the magnitudes of the outer line separations in Figs. 8 and 9.

The interpretation of the resonant CARS spectrum of OH in terms of third-order perturbation theory thus results in the prediction of a rather simple spectrum consisting of well-separated triplets. As has been emphasized by Druet and co-workers,[8] the perturbation expression (Eq. 1) for the third-order susceptibility will not be applicable if the pump or Stokes powers give rise to appreciable saturation. As will be seen, there is evidence of saturation in the experimental spectra obtained in these investigations, and this may preclude a simple interpretation of the experimental results. Under such conditions, corrective terms can, in principle, be applied (Druet, et al. [8]). But a better theoretical approach might be along the lines of the analysis of strong-field effects in CARS by Wilson-Gordon, Klimovsky-Baird, and Friedmann.[17] They perform a full solution of the density matrix equation of motion for a three level system, and obtain analytical solutions in var-

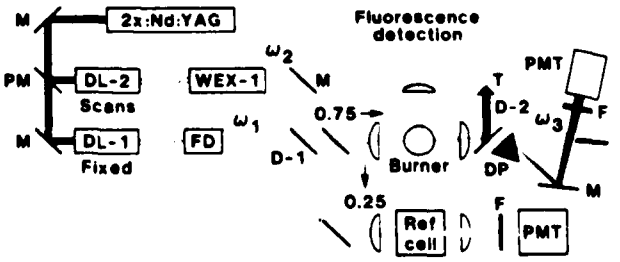

Fig. 10 Schematic diagram of the resonant CARS experiment. Symbols are described in the text.

ious limiting situations. Equally important is the question of collisional redistribution of population. As will be seen, the experimental results do confirm the basic triplet structure, but there is additional satellite structure around each basic component of the triplet that is suggestive of collisional transfer to adjacent rotational states. The question thus arises as to whether rotational redistribution within the upper A state and/or collisional electronic quenching to the ground X state could give rise to extra coherences. This problem may have connections with the "pressure-induced extra resonances" that have been predicted and observed by Prior, et al.[18] An interpretation of these extra resonances has been carried out by Grynberg,[19] who employs the formalism of the "dressed atom". These effects are areas of future investigation and are in the forefront of resonant CARS theoretical research.

Experimental

Several important factors must be carefully considered in the design of a resonant CARS experiment which attempts to detect a molecular free radical in the gas phase. The problems are compounded by the fact that the OH electronic transitions lie in the ultraviolet. The requirement of working in the UV introduces the additional complexities of frequency doubling two narrowband tunable dye lasers, working exclusively with fused silica optics, manipulating and detecting ultraviolet beams, and dealing with dichroic mirrors and filters that are only partially effective in re-

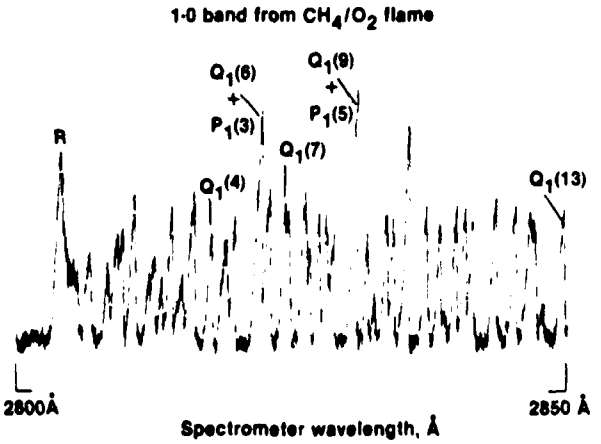

Fig. 11 OH emision spectrum employed for calibration purposes.

jection of unwanted wavelengths, while at the same time, severely attenuating the desired wavelength.

The configuration conventionally employed for resonant CARS makes use of two tunable, narrowband dye lasers whereby the ω_1 laser is tuned to a selected electronic resonance and held fixed, and then slowly scanning the Stokes laser, ω_2, which generates the resonant CARS spectrum, ω_3. The experimental configuration employed at UTRC is shown schematically in Fig. 10. The two tunable narrowband dye lasers, DL-1 and DL-2, are synchronously driven with the second harmonic (532 nm) of a Quanta-Ray pulsed neodymium YAG laser (DCR-1) operating at 10 Hz. The partial mirror (PM) allots about 40 percent of the 532 nm radiation to a commercial pulsed dye laser (Quanta-Ray PDL-1), denoted DL-2, and the remaining portion to a homemade dye laser (DL-1) of the Littmann grazing-grating configuration.[20] Each dye laser consists of side-pumped oscillator and preamplifier stages, followed by an end-pumped amplifier stage. Each dye laser produces laser radiation of frequency width less than 0.1 cm^{-1} and energy per pulse between 10 and 20 mJ, depending upon the laser dye chosen.

As stated previously, the outputs from both dye lasers must be frequency doubled. For the ω_1 laser, frequency doubling is a trivial task and requires only a manually adjustable second harmonic crystal, FD, in the figure. However, because ω_2 is scanned, an automatic angle-tuned device which maintains constant output power of the second harmonic frequency as the fundamental is tuned, must be employed. A WEX-1(Quanta-Ray) performs this task over the fundamental dye laser spectrum at scan rates in excess of 0.05nm/s. Second harmonic conversion efficiency appears to be about 10 % for both lasers; hence, ultraviolet energies are between 1 and 2 mJ per pulse, which corresponds to peak powers of 100 to 200 kW.

The two ultraviolet beams are combined with a dichroic mirror and focussed into the flame in the collinear CARS configuration. The beams emerging from the flame, now containing the CARS frequency also, are recollimated and directed to the detection system. ω_1 and ω_2 are partially removed with the dichroic D-2 and trapped in the trap, T. Because the dichroic is unsuccessful in completely removing ω_1 and ω_2 from ω_3, the three beams are spatially separated with the dispersing prism, DP. The unwanted beams are masked out and ω_3 is allowed to enter a filtered photomultiplier, PMT. The reference cell leg of the experiment is derived by picking off 25 % of the incident beams and focussing into a high pressure cell and detecting the nonresonant(non-vibrationally resonant) CARS

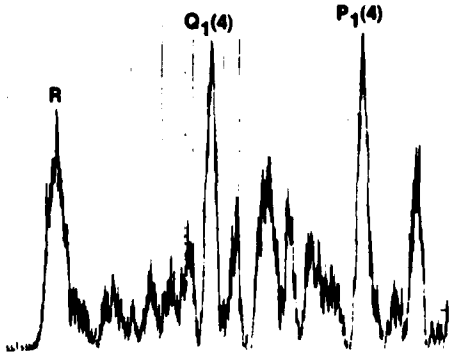

Fig. 12 Laser-induced fluorescence spectrum for ω_1 tuned to the $Q_1(4)$ line of OH.

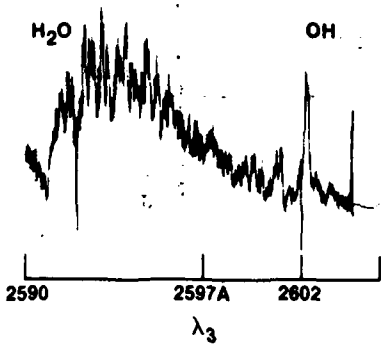

Fig. 13 First observation of resonant CARS in the OH radical. ω_1 tuned to resonance on $P_1(9)$.

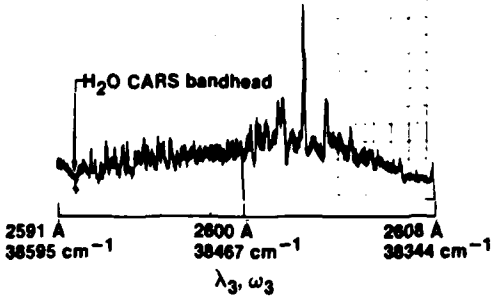

Fig. 14 Resonant CARS spectrum obtained for ω_1 tuned to $Q_1(14)$.

signal. Unfortunately the reference cell leg did not functions as well as anticipated, hence all the CARS spectra displayed below are uncorrected for laser power variation and dye laser profile.

A most essential feature of the experiment is the emission/fluorescence detection arm shown perpendicular to the CARS beams, above the burner, in Fig. 10. This portion of the experiment serves to calibrate a monochromator through the emission spectrum of OH from a methane/oxygen

flame, obtained with the aid of a chopper and lock-in detector. As as example, a portion of the 1-0 emission from OH over a 50 A span is shown in Fig. 11. A few of the rotational lines are identitfied for illustration. More importantly, this subsystem serves to both indicate when resonance excitation is achieved, and to identify the particular transition which is resonant. This is done by recording the laser-induced fluorescence through use of a boxcar integrator following the monochromator-PMT. The LIF spectrum for ω_1 exciting the $Q_1(4)$ line of the 1-0 band of OH is shown in Fig. 12. This type of spectrum, much different from the emission spectrum, clearly and uniquely indentifies the resonance on $Q_1(4)$ because of the strong fluorescence from $P_1(4)$.

The burner used throughout these studies consisted of a staggered array of stainless steel capillary tubes(0.125 in o.d.) which were ground flush with an edge-cooled brass plate which held the tubes in place. The matrix of alternating fuel/oxidizer tubes was surrounded by an outer layer of tubes which provided a nitrogen sheath to stabilize the flame. During the course of this investigation, a methane-oxygen flame has been used rather than the more tempermental hydrogen/oxygen flame. This type of burner produces a flame which is very uniform in appearance. The burner is mounted on a translation stage which can be moved in the vertical direction so that the CARS laser beams can be varied in height relative to the burner surface.

Resonance CARS Results

The first demonstration of resonant CARS in OH was obtained with ω_1 resonant on the $P_1(9)$ line of the 1-0 vibronic band. The spectrum is shown in Fig. 13. This type of spectrum (a scanned CARS spectrum) is obtained by scanning the ω_2 dye laser, while recording the change in intensity of the ω_3 signal falling on the detector. The region of the spectrum to the left is the water CARS spectrum which is not an electronically resonant spectrum. However, because of the great abundance ot water vapor in this flame, the "normal" CARS spectrum is easily observed. The sharp rise occurring around 2591 A is the bandhead of the water CARS spectrum. The resonant CARS of OH, occurring in the tail of the water CARS spectrum, has its strongest peak at 2602 A and represents a case where ω_1 has not been precisely tuned to the center of resonance. In contrast the resonant CARS spectrum of OH with ω_1 carefully tuned to the $Q_1(14)$ line (adjacent to the $P_1(9)$) is shown in Fig. 14. For this case, the water CARS spectrum is barely discernible, while the OH lines are

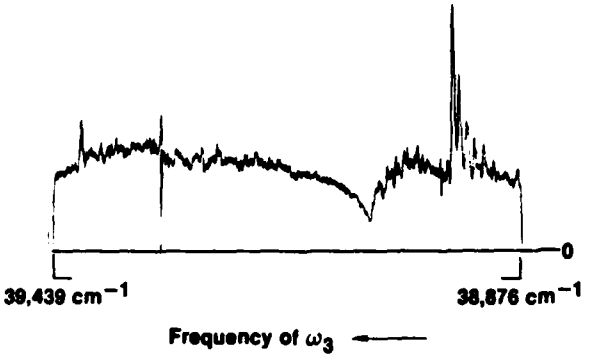

Fig. 15 Wide frequency scan of resonant CARS spectrum for resonance on $Q_1(4)$.

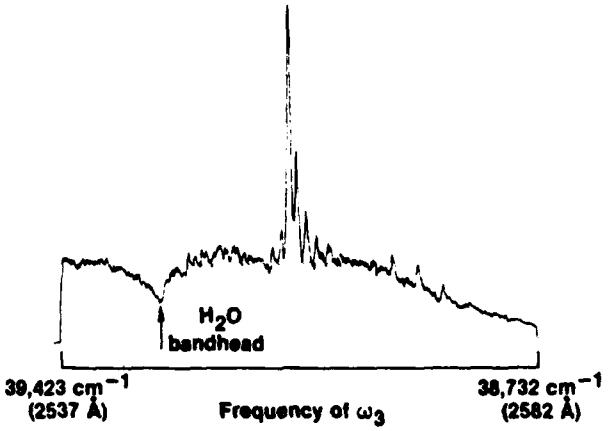

Fig. 16 Resonant CARS spectrum for ω_1 tuned to $Q_1(2)$.

much stronger, at least 5 times stronger. This is good evidence that resonant CARS is being observed, because the water concentration is at least four to five times that of OH in the CH_4O_2 flame, and because CARS signals scale as concentration squared, the normal CARS of OH would be less than 0.1 that of the H_2O CARS signal. In other words, it would be nearly totally lost in the water CARS band. The enhancement factor for the OH resonant CARS may even be larger than is apparent, because the true scaling of the CARS signal involves a consideration of linewidths and constructive/destructive interferences between lines.

The resonant CARS spectra obtained for the $P_1(9)$ and $Q_1(14)$ reonances are incomplete with respect to the predicted CARS spectra of Figs. 8 and 9. They are incomplete

in the sense that the outermost lines are not observed in the experiment, because of the limited spectral tuning range of ω_2. The spacing between these components is $2B(2J + 1)$ where B is the rotational constant for OH, approximately 19 cm^{-1}. Hence, for high J values, the separation can be several hundred wavenumbers and far beyond the tuning range of a single laser dye. For these reasons, it was decided to move ω_1 toward resonances with lower J values, namely, $Q_1(4)$ and $Q_1(2)$. Examples of resonant CARS spectra for these two cases are shown in Figs. 15 and 16 respectively. As may be seen, the scans cover a reasonably wide frequency range, in excess of 300 cm^{-1}. For the case of the $Q_1(4)$ spectrum, considerable structure may be seen to the left of the water CARS bandhead. These lines have not yet been identified as positively originating from OH, however. For the $Q_1(2)$ resonance CARS, some structure is observed to the right of the strong central OH resonant CARS band, at approximately the proper spacing. This structure does not consist of a single line, but also exhibits some satellite lines, contrary to theoretical prediction.

A preliminary exploration of saturation was made by reducing the intensity of the ω_1 beam with fused silica flats and partially reflecting UV mirrors. The maximum attenuation so obtained was a factor of 5.5. In order to obtain a reasonable signal strength at this level of attenuation, the PMT supply voltage was increased. The results of this test are shown in Fig. 17. Note that there is a considerable change in the shape of the OH spectrum and in the number of lines. Note also that the water CARS spectrum is barely discernible in the attenuated ω_1 spectrum. The increased gain required to maintain the same signal level was approximately 10; because the CARS signal scales as the square of the ω_1 power, a reduction of about 30 should have been seen. This observation, along with the change in shape is evidence that saturation must be considered. A more thorough study is called for; one which also includes attenuation of the ω_2 laser beam to determine if both laser beams can contribute to saturation of the resonant CARS process.

Finally, an initial study of the sensitivity of the resonant CARS spectrum to changes in concentration was performed by changing the height of the incident CARS laser beams relative to the height of the burner surface. The results are shown in Fig. 18, where spectra for 0.5 cm increments are displayed. The scans shown cover just the spectral region of the water and OH CARS bands. Clearly, the OH concentration decreases as the CARS beams are moved

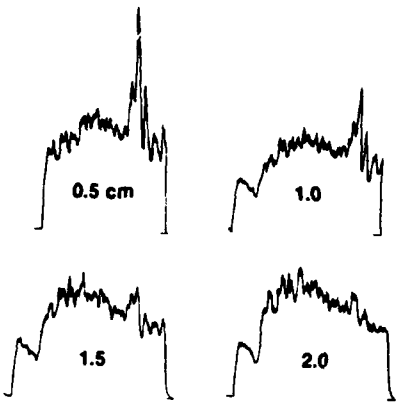

Fig. 18 Variation of the resonant CARS spectrum with change in laser beam height relative to burner surface.

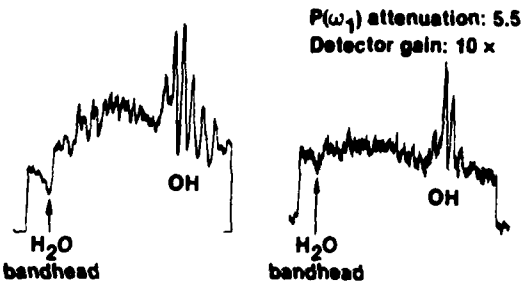

Fig. 17 Change in the resonant CARS spectrum with attenuation of the ω_1 intensity.

away from the burner surface; at the same time, the water concentration appears to be increasing slowly. At the largest separation, 2 cm, there is still some indication of OH, as a modulation on the background. Future studies will involve a detailed calibration of the concentrations of both OH and water throughout the flame, as well as the temperature distribution, so that resonant CARS as a quantitative diagnostic may be properly assessed. Saturation may prove to be a problem for quantitative measurements; however, even in the case of saturation, it may be possible to construct a working curve of concentration vs signal strength.

Conclusions

Electronically resonant CARS of the OH radical has been demonstrated in a very hot methane/oxygen flame. The resonant CARS spectrum was generated by use of two frequency-doubled, pulsed, narrowband dye lasers, one of which

was tuned and then fixed on a selected OH X-A transition, while the other other was scanned over the appropriate range. The OH resonant CARS signal is strong compared to the water CARS spectrum, even though water is much more abundant than OH in the flame. Resonant CARS was observed for several different electronic resonances and was quite sensitive to precise tuning of the ω_1 frequency. The theory of resonant CARS in the OH radical has been treated and the predicted appearance of OH resonant CARS spectra presented. Saturation, for which there is some experimental evidence, has not been included in the theory. Agreement between theory and experiment is good, except for the experimental observation of satellite structure about the central line. This additional structure is believed to arise from collisional redistribution of population in rotational energy levels of the upper electronic state. The variation of the resonant CARS spectrum as a function of laser beam height in the flame was observed and offers promise that resonant CARS may be applicable to quantitative measurements. Future studies will involve refinement of the theory to include saturation. Further experimental work will assess the feasibility of making quantitative measurements in a flame, a thorough exploration of saturation effects, measurement of the resonance enhancement factor, and precise spectral line positions. Another interesing investigation which must be explored is that of pressure-induced extra resonances, which may occur in four-wave mixing processes such as CARS, a so-called PIER-4 process.[18] Additionally, triple resonances will be searched for, if a theoretical survey suggests that promising possibilities exist in OH.

Acknowledgments

The authors wish to acknowledge valuable discussions with Prof. Nicolaas Bloembergen of the Harvard University Physics Department and with Dr. D. R. Crosley of SRI International. Thanks are also due Edward Dzwonkowski and Normand Gantick for assistance with the experiments. The authors especially wish to thank the United States Air Force Office of Scientific Research for partial support of this research through Contract No. F49620-81-C-0063.

References

[1]Eckbreth, A.C., and Hall, R.J. "CARS Thermometry in a Sooting Flame," Combustion and Flame, Vol. 36, March, 1979, pp. 87-98.

[2]Pealat, M., Taran, J-P.E., Taillet, J., Bacal, M., and Brunetau, A.M., "Measurement of Vibrational Populations in Low-pressure Hydrogen Plasma by Coherent Anti-Stokes Raman Scattering," Journal of Applied Physics, Vol.53, April, 1981, pp. 2687-2691.

[3]Stenhouse, I.A., Williams, D.R., Cole, J.B., and Swords, M.D., "CARS in an Internal Combustion Engine," Applied Optics, Vol. 18, 15 November, 1979, pp. 3819-3825.

[4]Eckbreth, A.C., Dobbs, G.M., Stufflebeam, J.H., and Taylor, P.A., "CARS Temperature and Species Measurements in Augmented Engine Exhausts," AIAA Paper No. 83-1294, presented at the AIAAASME-SAE 19th Joint Propulsion Conference, Seattle, Washington, June 27-29, 1983.

[5]Druet, S., and Taran, J-P.E., "Coherent Anti-Stokes Raman Spectroscopy," in Chemical and Biological Applications of Lasers, C.B. Moore, Ed., Academic Press, New York, 1979, pp. 187-252.

[6]Tolles, W.M., Nibler, J.W., McDonald, J.R., and Harvey, A.B., "A Review of the Theory and Application of Coherent Anti-Stokes Raman Spectroscopy(CARS)," Applied Spectroscopy, Vol. 31, July-August 1977, pp. 253-272.

[7]Verdieck, J.F., Shirley, J.A., Hall, R.J., and Eckbreth, A.C., "CARS Thermometry in Reacting Systems," in Temperature, Its Measurement and and Control in Science and Industry, American Institute of Physics, New York, 1982, pp. 595-608.

[8]Druet, S., Attal, B, Gustafson, T.K., and Taran, J-P.E., "Electronic Resonance Enhancement of Coherent Anti-Stokes Raman Scattering," Physical Review A, Vol. 18., October 1978, pp 1529-1557.

[9]Guthals, D.M., Gross, K.P., and Nibler, J.W., "Resonant CARS Spectra of NO_2," Journal of Chemical Physics, Vol. 70, March, 1979, pp. 2393-2398.

[10]Attal, B., Debarre, D., Muller-Dethlefs, K., and Taran, J-P.E., "Resonance Enhanced Coherent Anti-Stokes Raman Scattering in C_2 " Revues des Physique Appliquee', Vol. 18, p 39-50, January, 1984.

[11]Crosley, D.R., "Collisional Effects on Laser-Induced Fluorescence Flame Measurements," Optical Engineering ., Vol. 20, July-August 1981, pp. 511-521.

[12]Dieke, G.H., and Crosswhite, H.M.,"The Ultraviolet Bands of OH" Journal of Quantitative Spectroscopy and Radiative Transfer, Vol. 2, December 1962, pp. 97-199.

[13]Bloembergen, N., Lotem, H.L., and Lynch, R.T., "Lineshapes in Coherent Resonant Raman Scattering," Indian Journal of Pure and Applied Physics, Vol. 16, May 1978, pp. 151-158.

[14]Coxon, J.A., "Optimum Molecular Constants and Term Values for the X and for A States of OH," Canadian Journal of Phyics, Vol. 58, February 1980, pp. 933-949.

[15]Chidsey,I.L., and Crosley, D.R., "Calculated Rotational Transition Probabilities for the A-X System of OH," Journal of Quantitative Spectroscopy and Radiative Transfer, Vol. 23, March 1980, pp. 187-199.

[16]Earls, L.T., " Intensities in $^2\Pi$ - $^2\Sigma$ Transitions in Diatomic Molecules," Physical Review, Vol. 48, November 1935, pp. 423-424.

[17]Wilson-Gordon, A.D., Klimovsky-Baird, R., and Friedmann, H., "Saturation Effects in Coherent Anti-Stokes Raman Scattering," Physical Review A., Vol. 25, April 1982, pp. 1580-1595.

[18]Prior, Y., Bogdan, A.R., Dagenais, M.W., and Bloembergen, N., "Pressure Induced Extra Resonances in Four-Wave Mixing," Physical Review Letters, Vol. 46, January 1981, pp. 111-114.

[19]Grynberg. G., "Resonances Between Unpopulated Levels in Non-Linear Optics," Journal of Physics D., Vol. 14, May 1981, pp. 2089-2097.

[20]Littman, M.G., and Metcalf, H.J., " Spectrally Narrow Pulsed Dye Laser Without Beam Expander," Applied Optics, Vol. 17, July 1978, pp. 2224-2227.

END

FILMED

6-85

DTIC